UNCLASSIFIED

Y-1413
Metals, Ceramics & Materials

AEC RESEARCH AND DEVELOPMENT REPORT

THE DESIGN AND PERFORMANCE OF LEVITATION MELTING COILS

W. J. Hulsey

UNION CARBIDE NUCLEAR COMPANY
DIVISION OF UNION CARBIDE CORPORATION

Operating

- OAK RIDGE GASEOUS DIFFUSION PLANT
- OAK RIDGE Y-12 PLANT
- OAK RIDGE NATIONAL LABORATORY
- PADUCAH GASEOUS DIFFUSION PLANT

for the Atomic Energy Commission

Under U. S. Government Contract W7405 eng 26

UNION CARBIDE

UNCLASSIFIED

Printed in USA. Price: $1.75 Available from the
Office of Technical Services
U. S. Department of Commerce
Washington 25, D. C.

Date Issued: April 26, 1963

Report Number Y-1413

Metals, Ceramics and Materials
TID-4500 (19th Edition)

UNION CARBIDE NUCLEAR COMPANY
Division of Union Carbide Corporation

Y-12 PLANT

Contract W-7405-eng-26
With the U. S. Atomic Energy Commission

THE DESIGN AND PERFORMANCE OF LEVITATION MELTING COILS

W. J. Hulsey

This report is based on a study by the author as partial fulfillment of requirements for the degree of Master of Science in Metallurgical Engineering from the University of Tennessee.

Oak Ridge, Tennessee
March 5, 1963

Report Number Y-1413

Metals, Ceramics and Materials
TID-4500 (19th Edition)

Distribution:

Bailey, E. W.
Ballenger, H. F. (2)
Bernander, N. K.
Bunshah, R. F. (LRL)
Burditt, R. B.
Burkhart, L. E.
Cadden, J. L.
Comenetz, G. (Westinghouse R & D-Pittsburgh)
Cowen, D. D. (ORNL)
Evans, G. W.
Evans, P. A.
Fortenbery, M. J.
Friar, D. H.
Fultz, C. R.
Googin, J. M.
Gritzner, V. B.
Hackett, D. W.
Hamrin, C. E.

In addition, this report is distributed in accordance with the category, Metals, Ceramics and Materials as given in the "USAEC Standard Distribution Lists for Unclassified Scientific and Technical Reports", TID-4500 (19th Edition), February 1, 1963.

Harwell, W. L. (ORGDP) (5)
Hemperly, V. C.
Hemphill, L. F.
Henry, J. J.
Huber, A. P. (ORGDP)
Hulsey, W. J. (25)
Jackson, V. C.
Keller, C. A. (AEC-ORO) (4)
Kite, H. T.
Kobisk, E. H. (ORNL)
Lambert, F. J.
Lawson, C. G. (ORNL)
Lee, W. W., Jr.
Lewis, F. O. (ORGDP)
Little, J. C.
Lockhart, G. B.
Ludwig, R. L.
McHargue, C. J. (ORNL)
McLendon, J. D.
Mitchel, G. W.
Murray, J. P. (ORGDP)
Parker, G. I. (LEPEL)

Patterson, F. H.
Patton, F. S.
Phillips, L. R.
Picklesimer, M. L. (ORNL)
Pridgeon, J. W.
Rader, D. H.
Reece, J. S.
Roesch, C. J.
Schwenn, M. F.
Stansbury, E. E. (UT)
Stoner, H. H.
Tilson, F. V.
Uffelman, F. C.
Waters, J. L.
Whitson, W. K., Jr.
Wilkinson, P. E.
Winkel, R. A. (Paducah)
Wright, C. C.
Zurcher, E.
Y-12 Central Files (20)
Y-12 Central Files (Y-12RC)

ABSTRACT

Insufficient design information has limited the usefulness of the levitation melting process. This study was undertaken to evaluate the parameters involved in the performance of levitation coils with particular emphasis on the heating effect.

The field strength along the axes of various coils was measured using a small search coil, the voltage induced on this search coil being proportional to the field strength. The search coil was calibrated with a straight solenoid coil in which the field strength was calculated.

By considering each turn of a levitation coil as a short solenoid whose length was the tubing diameter, the field strength contribution from each turn was calculated. These values were summed along the axis to calculate the coil field. To aid these calculations, tables of field strength as a function of axial distance were prepared for various radii turns of different sizes of tubing.

The rate of increase of field strength along the coil axis per ampere of coil current was defined as the coil gradient. A parametric equation was derived relating the power input to a levitated sample to the coil gradient, sample size and resistivity, and frequency. The validity of this equation was checked by measuring the power input to levitated samples of various metals. The samples were coated with a temperature sensitive paint and heated at a constant power input. The power was calculated using the heat capacity and time to reach temperature.

The contribution from a given turn to the total coil gradient was calculated as a function of its location. This data was graphed with axial distance as

abscissa and turn radius as ordinate showing positions which give the same values of gradient contribution. The positions which contribute most to the coil gradient could be used to design coils of high gradient and, consequently, good heating efficiency.

Other results of the study include a possible method for measuring the surface tension of molten metals and a method for choosing the minimum frequency for efficient heating of a levitated sample.

TABLE OF CONTENTS

CHAPTER PAGE

LIST OF TABLES

LIST OF FIGURES

FIGURE PAGE

CHAPTER I

INTRODUCTION

I ADVANTAGES OF LEVITATION MELTING

Levitation melting has many advantages over more conventional laboratory melting techniques, particularly for reactive metals. Metals such as beryllium, titanium, and zirconium react with the most stable refractories, resulting in a loss of purity when crucibles are used for melting. Crucible melting of many less reactive metals is often undesirable when it is necessary to maintain ultra high purity. Arc melting in a cold copper crucible decreases this problem, although some copper contamination generally accompanies this technique. Melting in a cold crucible has the further disadvantage of temperature gradients in the melt producing segregation in alloys.

Levitation melting is not only useful in overcoming these difficulties but is often a more convenient technique even when satisfactory crucibles are available. The rapid melting cycle--often less than one minute--permits a large number of alloys to be prepared economically for many alloy investigations. After the sample melts, it is conveniently cast into the desired shape without special tilting or bottom pouring devices. Also, the absence of refractories in the coil system reduces the contamination of high-vacuum melting systems.

II OTHER USES

Levitation has applications other than alloy preparation. These uses include sintering, study of gas-metal reactions, and vapor plating (as evaporator source or substrate support). Measurements of the molten metal shape may also yield surface tension data (see Page 9).

III NEED FOR DESIGN INFORMATION

Although several investigators[1-13(Pages S10 and 273)] have used levitation melting successfully, they were limited to a few coil designs which were developed empirically with very little reference to electromagnetic field theory. This limitation has imposed serious restrictions on the quantity and kinds of metals which could be melted by this technique. Okress, Wroughton, Comenetz, Brace, and Kelly[7] performed an excellent analysis of the levitation forces on spherical shapes but they did not study the associated heating effects nor did they provide a direct approach to the problem of coil design. At present there is a need for simplified design information for use by the metallurgist who has only a casual knowledge of electromagnetic theory.

IV PURPOSE OF THIS STUDY

The purpose of this study was to provide a means for evaluating the various parameters involved in the design and performance of levitation coils. Particular

attention was paid to the heating effects during levitation, with only cursory treatment of the liquid support. The most important result of this investigation was the development of a simple expression for the power input to the levitated sample which involves a single coil parameter; viz., the rate of increase of the field strength along the coil axis. Methods for designing the coil were then developed using this parameter.

CHAPTER II

THEORY OF LEVITATION MELTING

I ELECTROMAGNETIC FIELD IN LEVITATION COIL

The flux lines of two coaxial coils carrying currents with 180-degree phase difference would appear somewhat as in Figure 1. At some point along the axis between the two coils the fields from each coil are equal and opposite such that they exactly counteract each other, producing a null point in the field. This null point is indicated in the figure as NP. The field strength increases in all directions from this point. For example, Figure 2 shows the field strength along the axis per ampere in the coil as a function of axial distance. The convention is used that the root-mean-square value of the field produced by the lower set of turns is positive and the opposite field of the upper turns negative. Of course, the field is alternating at high frequencies and will be a sine function of this value.

II INDUCED EDDY CURRENTS IN PART

If a conductor is placed in an alternating magnetic field, a voltage is induced around it having a magnitude equal to the time rate of change of the magnetic flux. This voltage produces a current which flows in a direction to produce an opposing flux. These are induced eddy currents which are responsible for the heating effect.

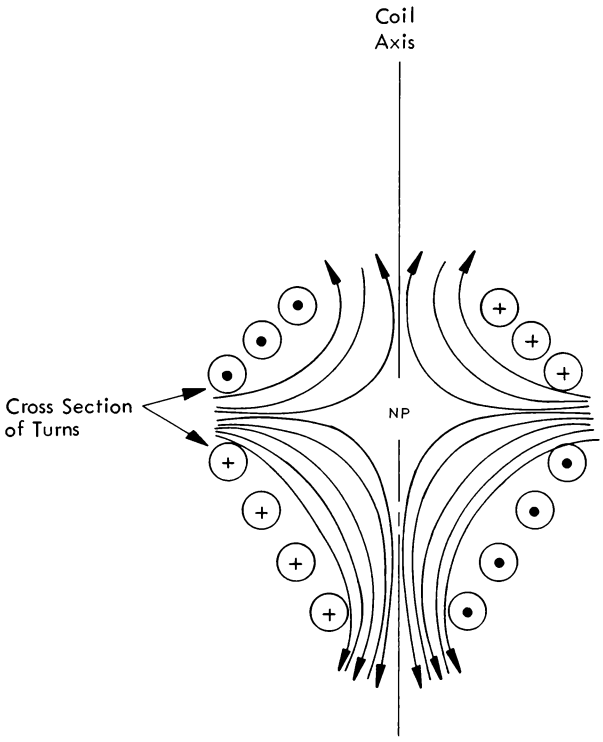

FIGURE 1

FLUX LINES IN LEVITATION COIL

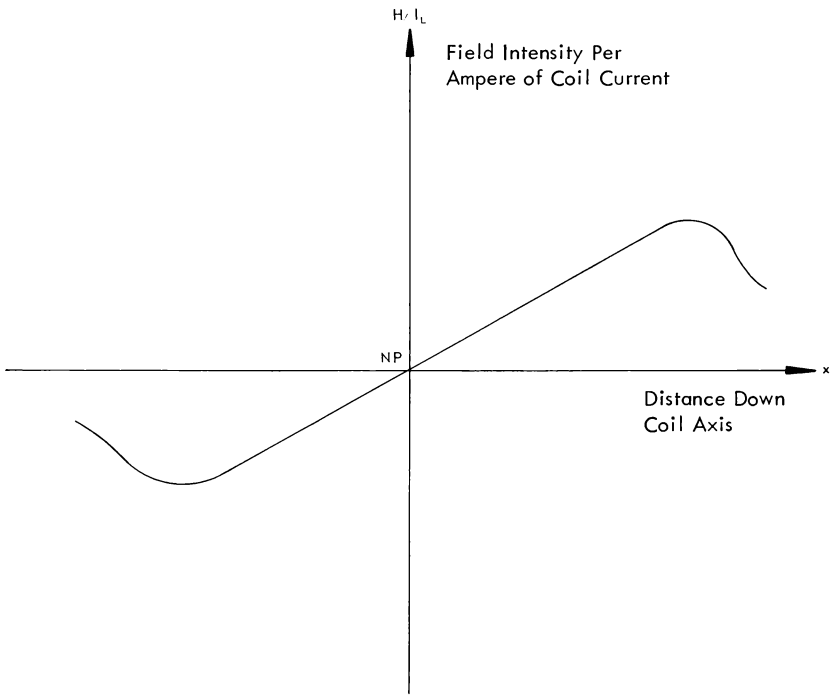

FIGURE 2

FIELD STRENGTH ALONG AXIS OF LEVITATION COIL

III REACTION BETWEEN EDDY CURRENTS AND FIELD

A force is exerted on a current-carrying conductor in a magnetic field in such a direction as to increase the energy stored in the magnetic field. Since the induced currents cause an opposing flux and consequently decrease the energy of the field, a force is exerted on the loop tending to move it out of the strong field. Since the weakest field in the levitation coil is at the null point, the current loops are all forced toward this point. The flux produced by the loop is a function of its area, so there arises a force which tends to "squeeze" the conductor even in a uniform magnetic field.

Another method of visualizing the origin of the levitating forces is to consider the interaction of small current elements with the surrounding magnetic field. When a current element is located perpendicular to a magnetic field, a force arises in a mutually perpendicular direction given by the familiar left-hand rule. The current loops around the levitated sample will react with the field in such a way as to produce forces normal to the flux lines. These forces will tend to compress the sample and move it toward the null point. These forces cause the molten sample to assume a shape similar to that shown in Figure 3. The shape will not conform exactly to the shape of the inducing field due to the distortion of the field by the eddy currents in the sample and because of the forces of gravity and surface tension which are also acting on the sample.

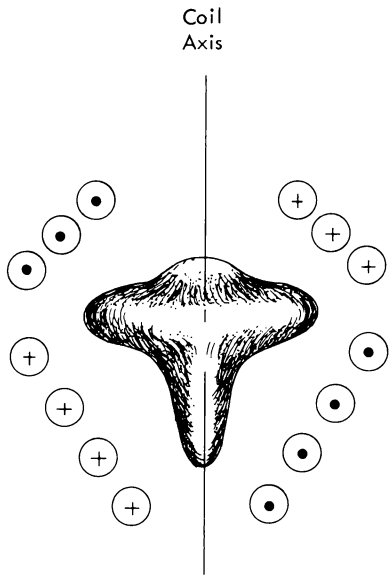

FIGURE 3

SHAPE ASSUMED BY LEVITATED MOLTEN METAL

IV ROLE OF SURFACE TENSION

It has been suggested[3,4,5,7,11,13(Page 273)] that the surface tension and density of liquid metals determine their tendency to drip from the levitated state. If it is assumed that the levitating forces on the bottom tip of the melt in the immediate vicinity of the coil axis are negligible, a relationship involving the surface tension and density can be derived.

Neglecting any electromagnetic or hydrodynamic forces on a very small column of liquid along the coil axis, the static equilibrium pressures can be equated. If the levitated sample has a density D_M and height h, gravity will cause a pressure hD_M at the bottom tip. The total pressure at the bottom tip would be the gravitational forces and the pressure exerted at the top of the column by the curvature of that surface. The pressure exerted by a curved surface of radius R and surface tension γ is given by

$$P = \frac{2\gamma}{R} \quad . \tag{1}$$

For equilibrium the surface tension pressure of the bottom tip curvature must just balance the downward pressure; thus

$$\frac{2\gamma}{r_B} = \frac{2\gamma}{r_T} + hD_M \quad , \tag{2}$$

where R_B and R_T are the radii of curvature of the bottom and top of the melt at the axis. This reduces to

$$\gamma = \frac{hD_M}{2}\left(\frac{r_T r_B}{r_T - r_B}\right) \quad . \tag{3}$$

If the assumptions made are justified, this might provide a technique for measuring the surface tension of liquid metals.

CHAPTER III

EQUIVALENT RESISTANCE EQUATION

I DEFINITION

The concept of equivalent resistance provides a convenient means of expressing the heating of a workpiece in an induction coil. This imaginary resistance is defined as the ratio of the power developed in the work to the square of the coil current. An equation was derived relating this ratio to the shape of the charge, its electrical resistivity, a single coil parameter, and the frequency.

II DERIVATION OF EQUATION

The rate of increase of the field intensity per ampere of coil current with respect to the distance from the null point can be defined as the specific gradient G, so that

$$G \doteq \frac{\partial (H/I_L)}{\partial x} \quad . \tag{4}$$

Assuming G is a constant over the distance encountered by the levitated work, the flux density at a distance x from the null point would be given by

$$B = \mu I_L G x \quad . \tag{5}$$

Multiplying by the cross-sectional area of the work at this value of x, the total flux is

$$\phi = \pi r_w^2 B = \mu I_L G x \pi r_w^2 \quad . \tag{6}$$

The voltage induced on this element is, by Faraday's law,

$$E = \frac{\partial \phi}{\partial t} = \omega \mu I_L G x \pi r_w^2 \quad . \tag{7}$$

The frequency term results from the derivative of the flux which is proportional to $\sin \omega t$.

The assumption is made that the workpiece can be treated as a single, series R-L circuit having some effective voltage drop which is proportional to the current, gradient, and frequency as in Equation (7). The proportionality constant depends on the actual shape of the charge since it involves an average value of $x r_w^2$. Denoting this factor as a_1,

$$E_w = a_1 I_L G f \quad . \tag{8}$$

The effective depth of penetration, δ , of eddy current in a conductor is given by

$$\delta = 3.16 \sqrt{\rho / f} \quad . \tag{9}$$

For an element of the work of thickness Δx and effective radius r_w , as in Figure 4, we have a resistance

$$R = \frac{\rho 2 \pi r_w}{3.16 \sqrt{\rho / f} \ \Delta x} \quad . \tag{10}$$

Combining the constants and average value of $r_w / \Delta x$ into a factor a_2 , also depending on the shape of the work, the effective resistance of the simplified R-L circuit becomes

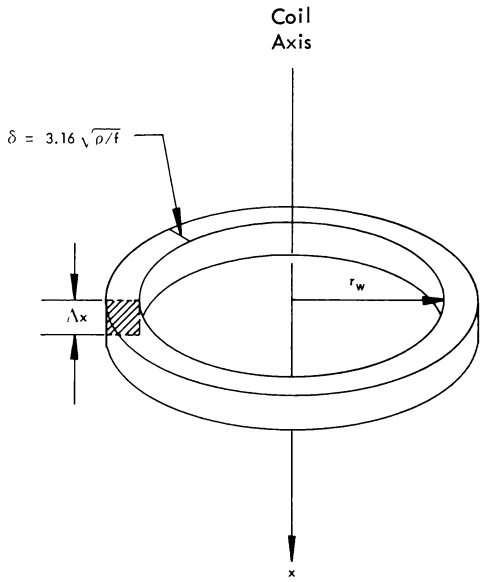

FIGURE 4

SEGMENT OF SURFACE OF LEVITATED SAMPLE REPRESENTING CURRENT-CARRYING LOOP

$$R_w = a_2 \sqrt{\rho f} \quad . \tag{11}$$

Further, assuming the effective inductance of the work is a function of the shape only, the inductive reactance is

$$X_w = 2\pi f L_w = a_3 f \quad . \tag{12}$$

The effective current in this R-L circuit is

$$I_w = \frac{E_w}{\sqrt{R_w^2 + X_w^2}} \quad , \tag{13}$$

which upon substitution gives

$$I_w = \frac{a_1 I_L G f}{\sqrt{a_2^2 \rho f + a_3^2 f^2}} \quad . \tag{14}$$

The power developed would be

$$P_w = I_w^2 R_w \quad , \tag{15}$$

or

$$P_w = \frac{a_1^2 I_L^2 G^2 f^2}{a_2^2 \rho f + a_3^2 f^2} \cdot a_2 \sqrt{\rho f} \quad , \tag{16}$$

or

$$P_w = \frac{I_L^2 G^2 \sqrt{\rho f} \quad f a_1^2 / a_2}{\rho + f a_3^2 / a_2^2} \quad . \tag{17}$$

Defining two shape factors as

$$S_1 \equiv a_1^2 / a_2 \; ; \quad S_2 \equiv a_3^2 / a_2^2 \quad , \tag{18}$$

Equation (17) becomes

$$P_w = I_L^2 \frac{S_1}{S_2} G^2 \sqrt{\rho f} \cdot \frac{1}{\rho/fS_2 + 1} \quad . \tag{19}$$

The equivalent resistance is defined as

$$R_{EQ} \equiv \frac{P_w}{I_L^2} \quad , \tag{20}$$

so

$$R_{EQ} = \frac{S_1}{S_2} G^2 \sqrt{\rho f} \; K \quad , \tag{21}$$

where

$$K \equiv \frac{1}{\rho/f S_2 + 1} \quad . \tag{22}$$

The factor K approaches unity as the frequency and shape factor S_2 increase or as the resistivity decreases.

III ANALOGOUS EQUATION IN LITERATURE

Tudbury[14] presented an equation for the equivalent resistance of a cylindrical workpiece in a straight solenoid which can be written as

$$R_{EQ} = F\sqrt{\rho f} \; K_R \quad , \tag{23}$$

where F is a function of the coil and workpiece geometry and K_R is a factor which approaches unity as the frequency and work diameter increase or as the resistivity decreases. The similarity of the frequency and resistivity dependence in Equations (21) and (23) is evident.

CHAPTER IV

EXPERIMENTAL VERIFICATION

The validity of Equation (21) was checked by measuring the power input to samples of stainless steel, lead, aluminum, and copper in a coil of known gradient, coil current, and frequency.

I MEASUREMENT OF COIL CURRENT

The inductor current in a resonant parallel L-C tank circuit with a low series resistance is given by

$$I_L = E_0 \omega_0 C \ , \tag{24}$$

where E_0 is the voltage across the circuit, ω_0 is the resonant frequency, and C is the capacitance. A tank circuit ammeter was made for a 10-kilocycle (kc) motor generator system by fixing a probe coil between the bus bars leading to the levitation coil, the voltage induced on this probe being proportional to the current flowing in the bus. By measuring this voltage and the voltage across the tank circuit, the ammeter was calibrated with the use of Equation (24), given the resonant frequency and parallel capacitance. The calibration factors determined with several different levitation coils were found to agree within 10 percent.

II MEASUREMENT OF FIELD

The field strength along the axis of the levitation coils was measured by measuring the voltage induced on a small (1/8-inch O.D. x 1/8-inch long) probe coil

wrapped on the end of a small quartz tube. This was placed inside a larger tube which acted as a guide to align the probe. This probe coil was calibrated by measuring the induced voltages when placed inside a straight solenoid where the field strength was calculated.

The field strength per ampere on the axis of a solenoid is given by[16]

$$H/I_L = \frac{N}{2d}\left[\frac{d/2 + x}{\sqrt{r^2 + (d/2 + x)^2}} + \frac{d/2 - x}{\sqrt{r^2 + (d/2 - x)^2}}\right], \tag{25}$$

where N is the number of turns, d is the length, r is the inside radius, and x the axial distance from the center of the coil. A one-inch diameter by 3 1/16-inch-long solenoid was constructed with ten turns of 1/4-inch copper tubing. The field strength along the axis of this coil, measured with the probe coil, is plotted in Figure 5 along with the calculated values. The calibration factor was obtained from the peak value at the center of the solenoid.

Figure 6 shows the measured field strength along the axes of several typical levitation coils used in this experiment. The slopes of these curves are defined as the gradients of the coils. Notice how this slope remains reasonably constant for a considerable distance from the null point. This behavior is a fortunate consequence of the arrangement of typical levitation coils. If the upper and lower turns were separated more, this condition would no longer exist and some average value of gradient would have to be used in Equation (21). The largest samples which could be placed in these coils were within the linear field region such that the constant gradient assumption was justified.

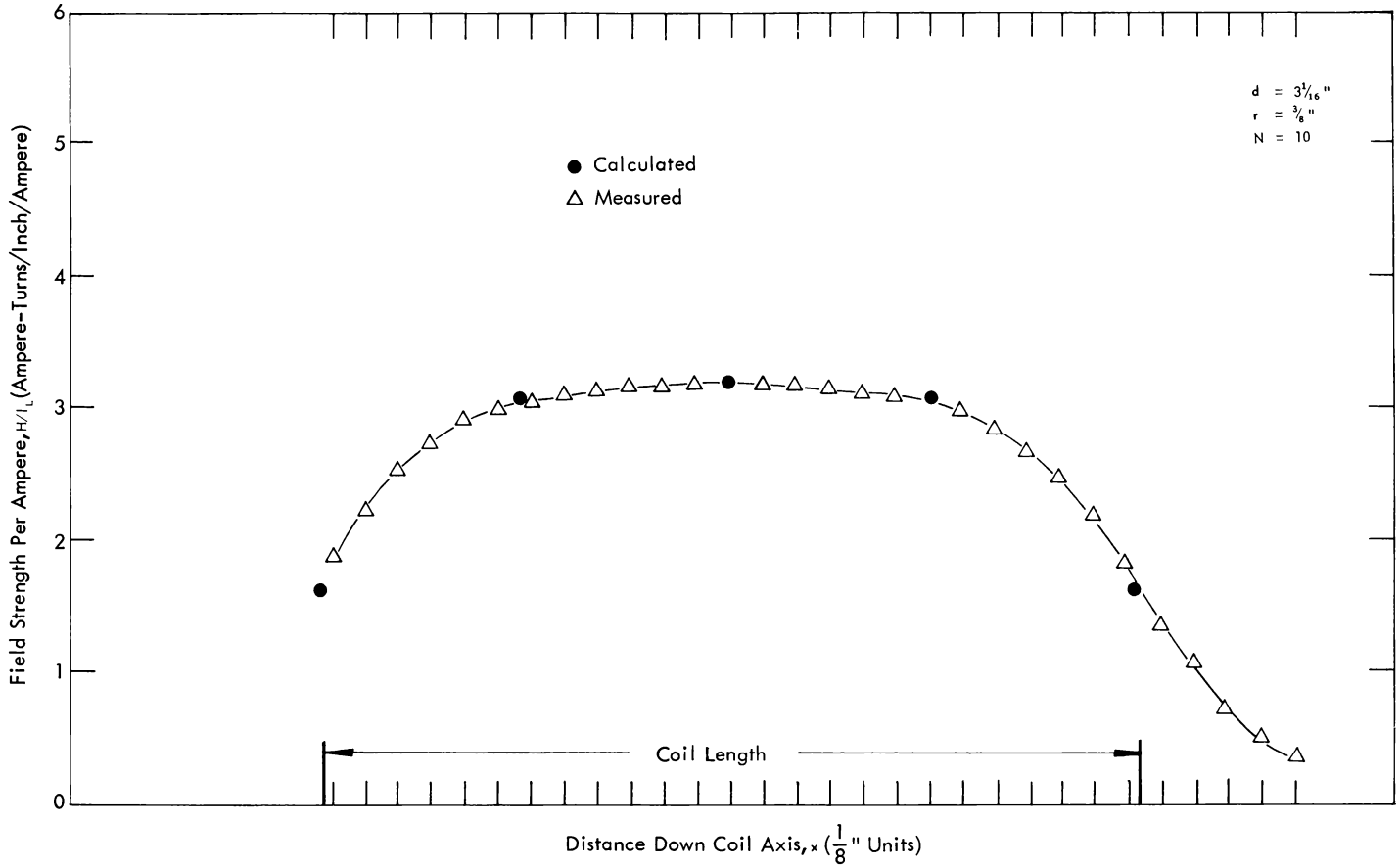

FIGURE 5

FIELD STRENGTH ALONG THE AXIS OF 3-INCH STANDARD SOLENOID

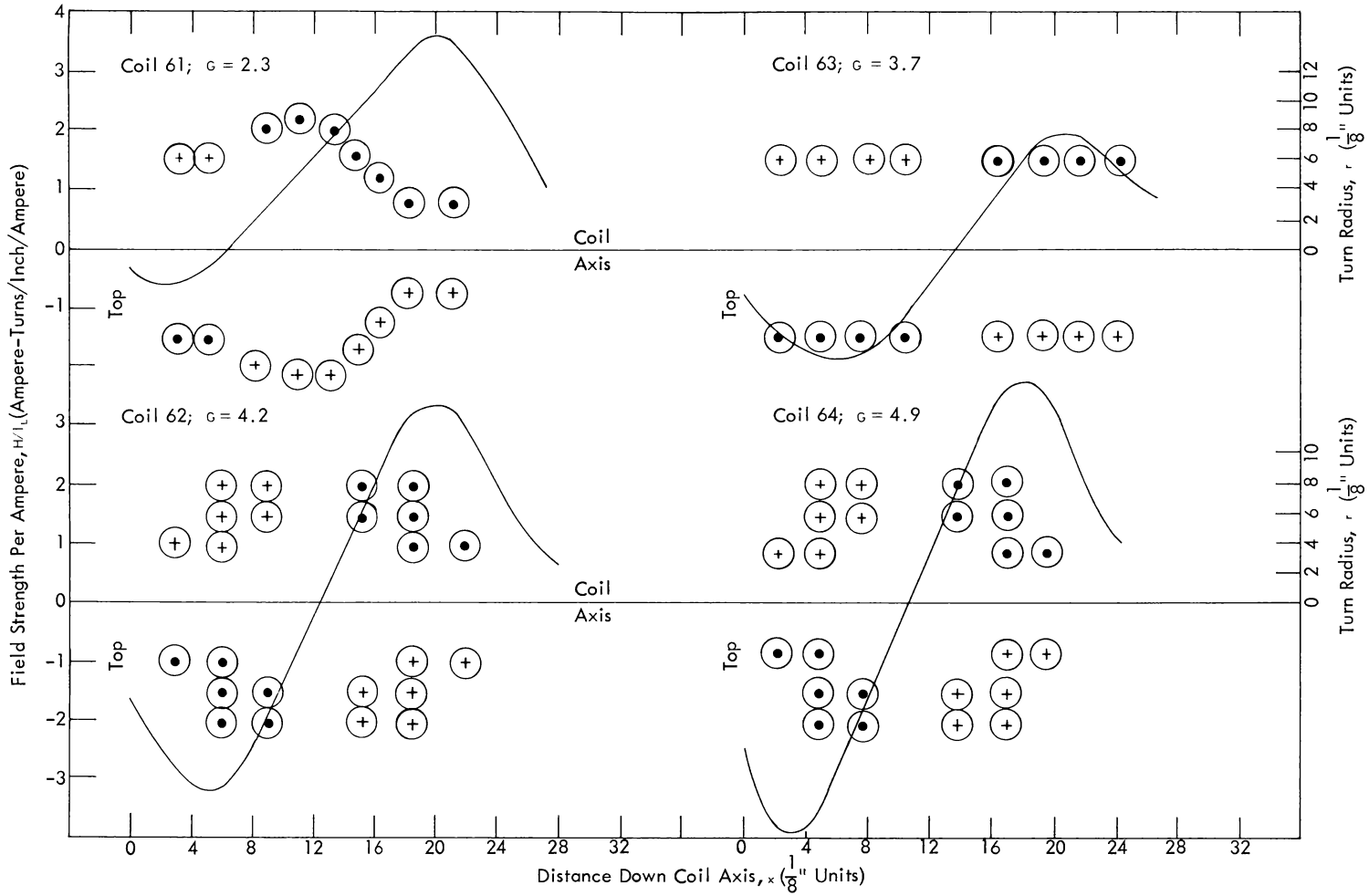

FIGURE 6

FIELD STRENGTH AND SHAPE OF COILS 61-64

III GRADIENT DEPENDENCE

Equation (21) contains only one coil parameter, G^2 . To test this hypothesis, the power input to identical samples of an aluminum alloy was determined for the four different levitation coils in Figure 6. The power was determined by measuring the time required to begin melting of the levitated sample for various coil currents. This time divided into the total enthalpy change gave the average power input. From the definition of R_{EQ} and Equation (21), the power input should be proportional to $I_L^2 G^2$ for constant shape, resistivity, and frequency. Figure 7 shows the experimental data. The ordinate intercept gives the average power loss from the samples. The increased values of P_w at low values of I^2G^2 result from the samples floating in positions appreciably below the null point, a condition not covered by Equation (21). This phenomenon has been reported in the literature[1-4] where the temperature of the levitated sample could be raised by lowering the coil current. With the coils tested in this experiment it was noted that a considerable sacrifice in stability was realized in using this increased coupling. Coil 61 was of the type most often reported in the literature and had more room for the sample to assume this low position. The low gradient of this coil caused a low efficiency even when the low-position heating was utilized.

IV FREQUENCY AND RESISTIVITY DEPENDENCE

Equation (21) can be rearranged to the form,

$$\rho/f = S_1 \frac{\sqrt{\rho f}}{R_{EQ}/G^2} - S_2 \quad , \tag{26}$$

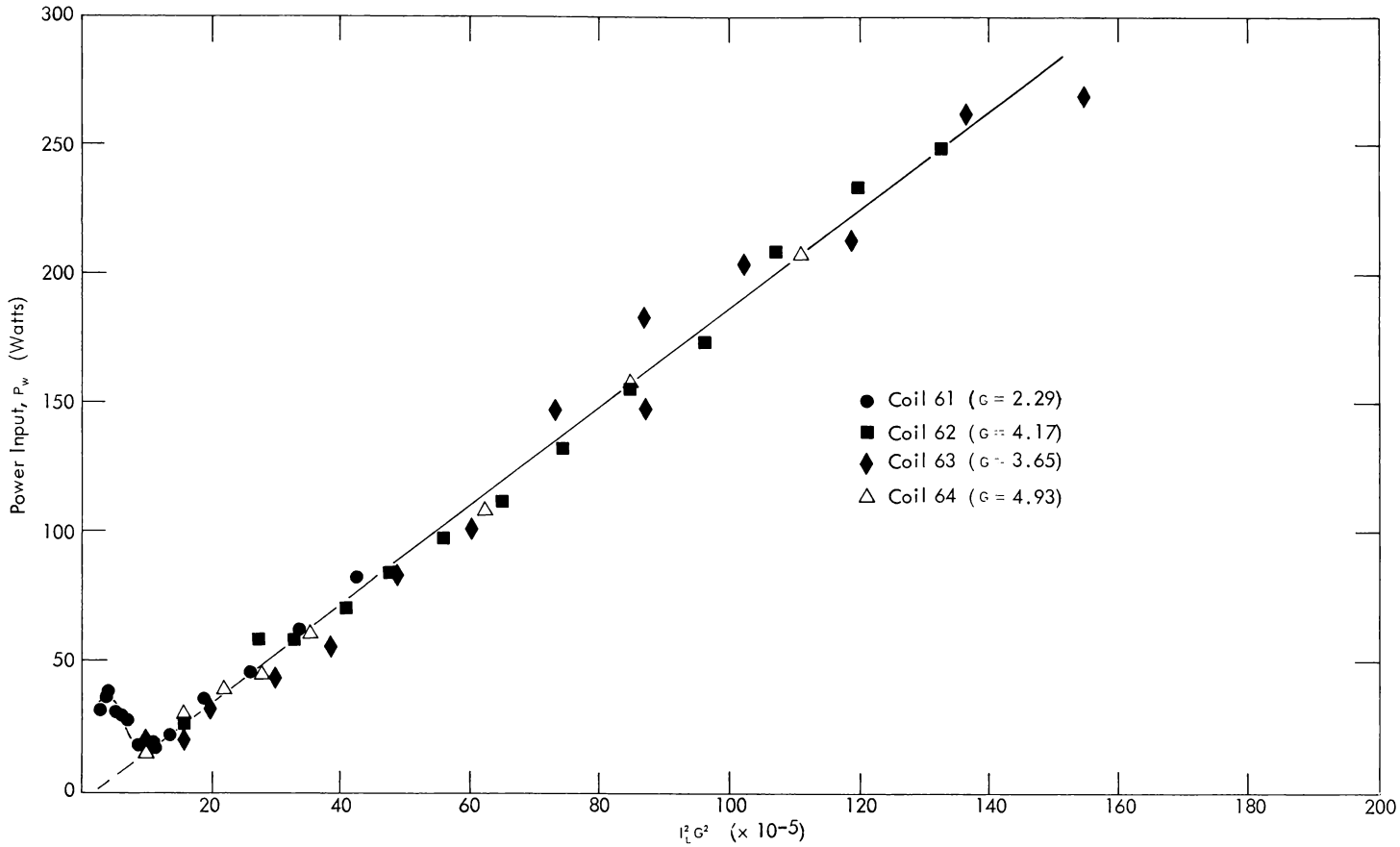

FIGURE 7

POWER INPUT TO 1-INCH DIAMETER X $\frac{1}{2}$-INCH-LONG SAMPLES OF 6061 ALUMINUM IN VARIOUS TYPE COILS

which predicts a straight line should be obtained when ρ/f is plotted against $\frac{\sqrt{\rho f}}{R_{EQ}/G^2}$ for samples of the same shape factors. Figure 8 shows the results of experiments in Coil 64 with 1-inch-diameter by 1/2-inch-long samples of four different materials tested at 10 kc and one at 520 kc.

The samples were coated with a temperature sensitive paint which melts at 204° C. By measuring the time required to reach this temperature and by knowing the specific heat, the average power input was calculated. It was necessary to aid the supporting of the heavier metals by spot welding or peening 0.020-inch wires into the surface in such a manner as to hold the sample in the position it would assume at higher coil currents. This allowed lower power inputs to the sample for more accurate measurements.

The fact that this data fits the straight line demonstrates the fact that R_{EQ} is indeed proportional to the ratio S_1/S_2 and the resistivity and frequency dependence is as given by Equation (21).

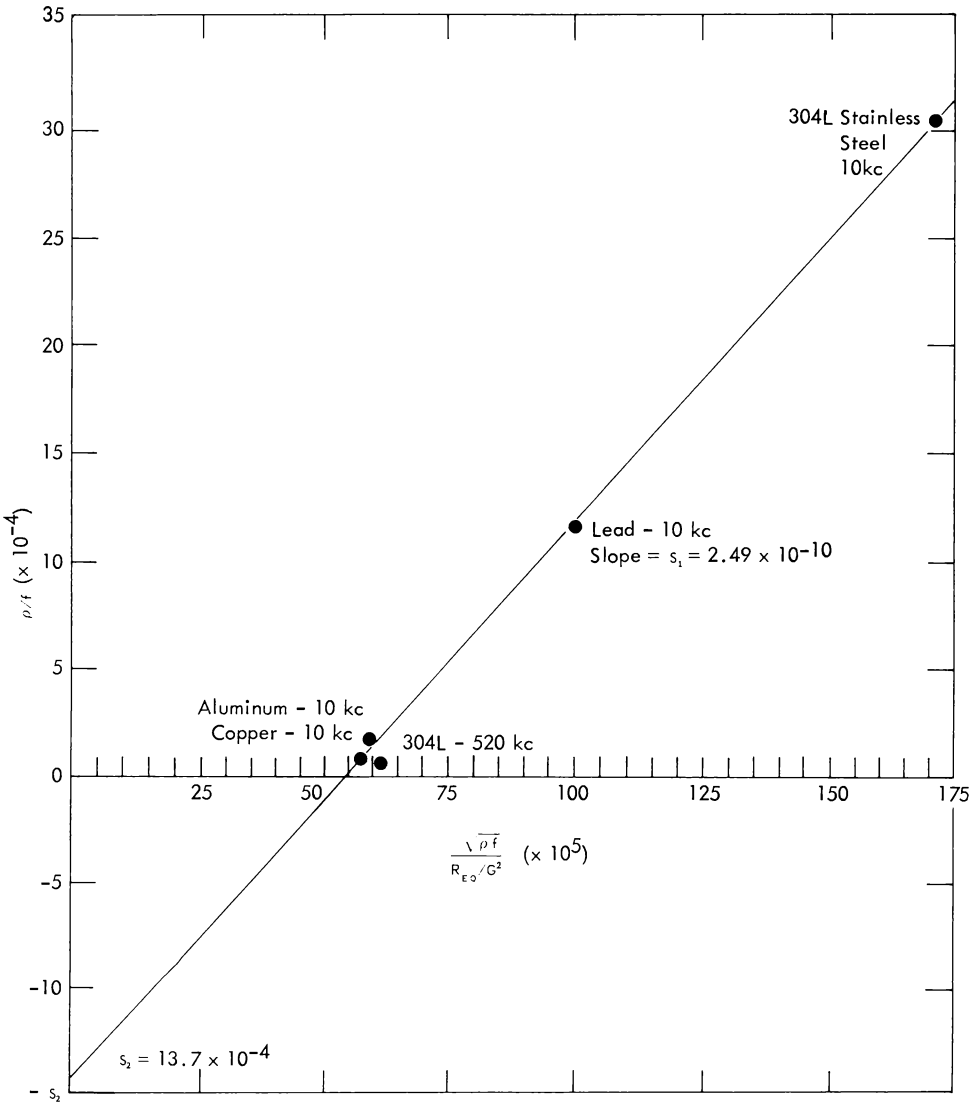

FIGURE 8

EVALUATION OF THE SHAPE FACTORS S_1 AND S_2 FOR 1-INCH DIAMETER BY $\frac{1}{2}$-INCH SAMPLES

CHAPTER V

APPLICATION OF EQUIVALENT RESISTANCE EQUATION

I EVALUATION OF SHAPE FACTORS

Before Equation (21) can be used to calculate the power input to a levitated sample, the shape factors s_1 and s_2 must be determined. Figure 8 provides an evaluation of the shape factors since the ρ/t intercept is s_2, the slope is s_1, and the inverse of the abscissa intercept is s_1/s_2. To ascertain the variation of these shape factors with size, determinations were made as above using 1100F aluminum and 304L stainless steel samples with 2:1 diameter to length ratios with diameter variations from 1/2 to 1 1/2 inches. As seen in Figure 9, both s_1/s_2 and s_2 are proportional to the fourth power of the diameter as

$$s_2 = 1.3 \times 10^{-3} D^4 \quad , \tag{27}$$

and

$$\frac{s_1}{s_2} = 2.0 \times 10^{-7} D^4 \quad . \tag{28}$$

This correlation, while sufficiently accurate for design applications, is not suitable for evaluation of the nature of the original factors a_1, a_2, and a_3. It should be noted that the equivalent resistance equation was derived on the basis of the assumption of current loops around the sample with no axial flow of current. In general, there will surely be a voltage gradient down the solid charge so that some

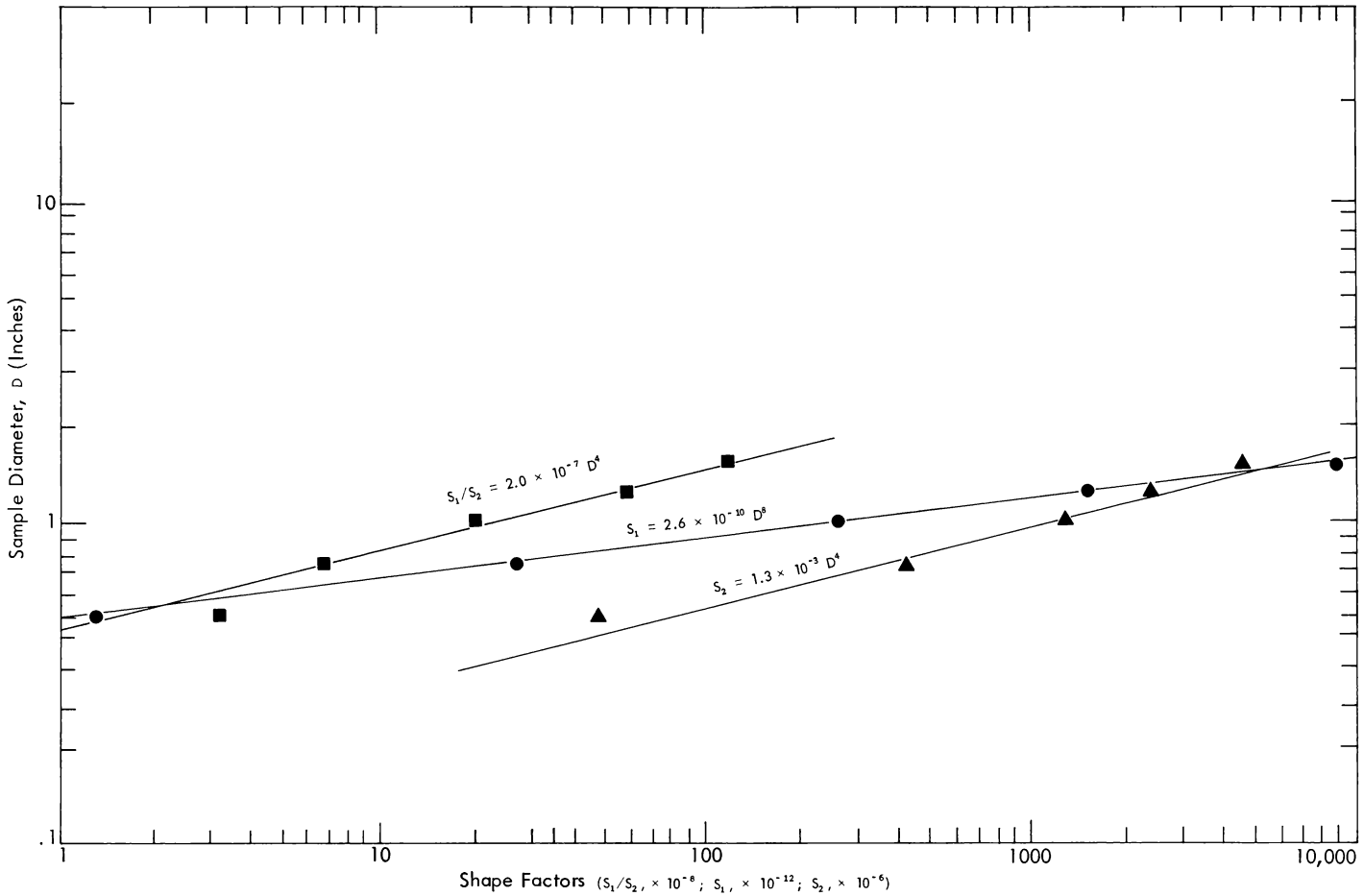

FIGURE 9

EVALUATION OF SHAPE FACTORS FOR 2:1 DIAMETER TO LENGTH RATIO

axial current flow must be present. This effect is evidently either very small or, probably, accounted for in the shape factors. This would make it very difficult to calculate the shape factors from the original sample geometry. Cursory attempts to explain the D^4 dependence of the shape factors from this basis were unsuccessful. Although the diameter to length ratio studied is a convenient one, evaluation of other shapes is in order for design information.

II FREQUENCY EFFICIENCY COEFFICIENT

The factor K might be termed an efficiency factor. The ratio of power input to the sample to the power developed in the coil is the ratio of the equivalent resistance to the coil resistance. This ratio is one measure of the heating efficiency. Since the high frequency coil resistance is proportional to the square root of the frequency, the only remaining frequency dependence of the resistance ratio is found in K. Thus, for any given frequency, size, and resistivity, K represents the fraction of the maximum possible efficiency which could be realized by increasing the frequency. For example, if $\frac{fS_2}{\rho}$ were equal to 0.5, K would have a value of 1/3 so the efficiency could be doubled by raising the frequency by a factor of four such that $\frac{fS_2}{\rho}$ would equal 2.0 and K equal 2/3.

III CHOICE OF FREQUENCY

As seen in Figure 10, the factor K increases rapidly up to a value of 0.75 and very slowly above this value. Thus, an increase in frequency when K is below

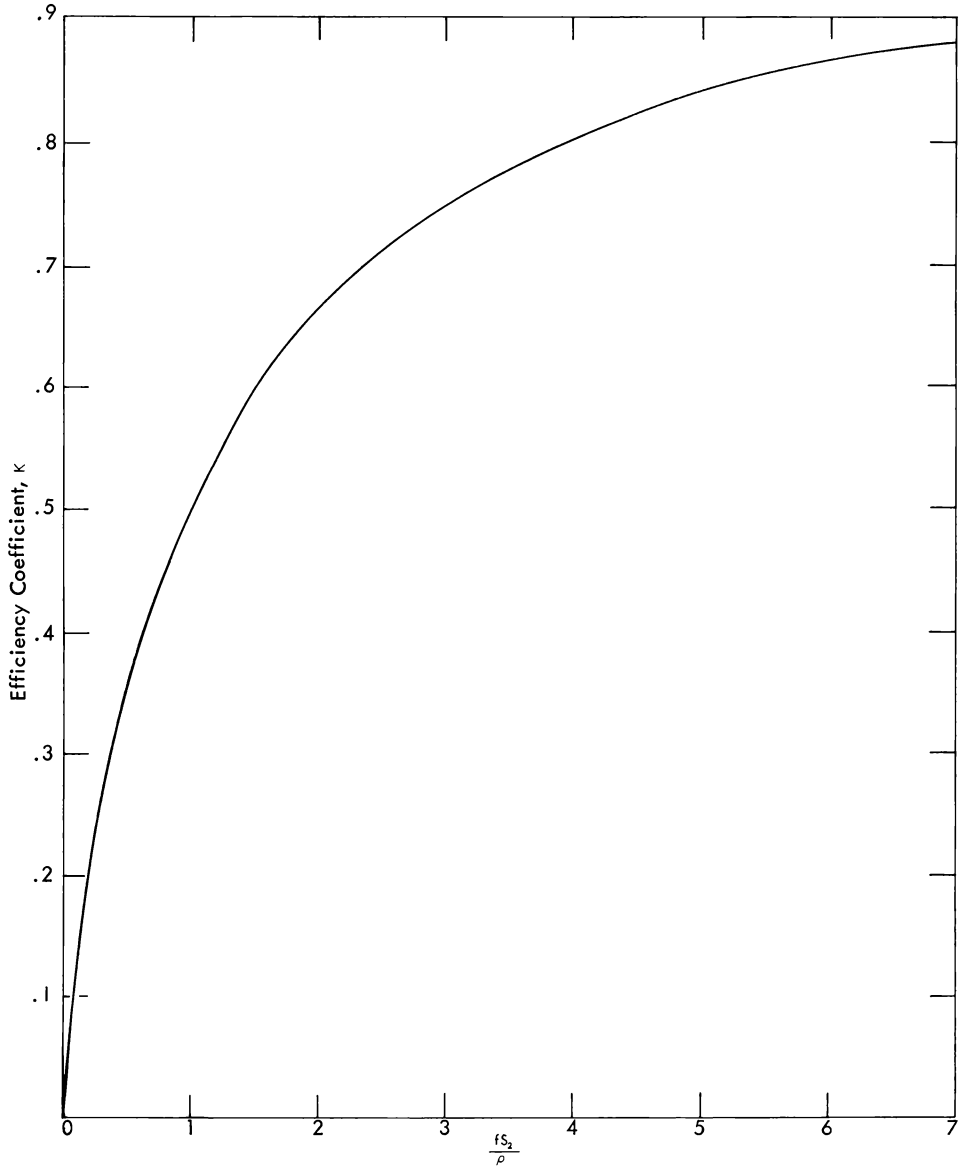

FIGURE 10

VARIATION OF THE EFFICIENCY COEFFICIENT

this value results in considerable increase in efficiency while little gain is realized when it is higher than 0.75. Figure 11 shows the frequency required for a K value of 0.75 for various resistivities and sizes for samples of 2:1 diameter to length ratio.

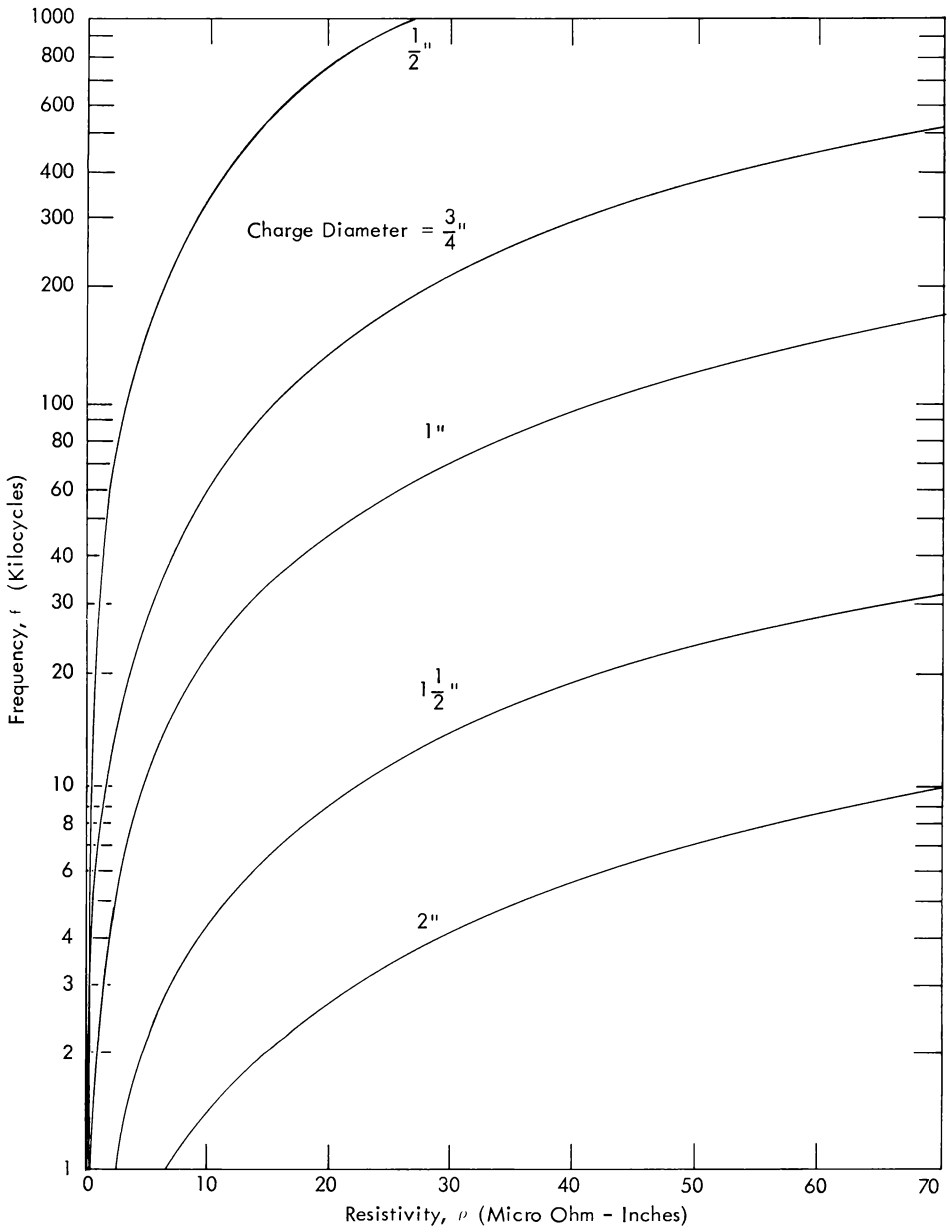

FIGURE 11

MINIMUM FREQUENCY FOR EFFICIENT HEATING OF A CHARGE WITH 2:1 DIAMETER TO LENGTH RATIO

CHAPTER VI

CALCULATION OF FIELD

I EQUATION

By considering each turn of a levitation coil as a single turn solenoid of length d, Equation (25) was used to calculate the contribution of each turn to the total field strength along the axis of the coil. Tables I, II, and III were computed from this equation for three sizes of tubing. Figure 12 shows the field contributions from 1/4-inch tubing. Figure 13 shows the variation due to different tubing sizes.

II SUPERPOSITION PRINCIPLE

By the principle of superposition the total field intensity at any point on the axis of a coil can be calculated by summing the contributions from the various turns taken from the table at the appropriate values of r and x. By convention the upper turns will make a negative contribution. This summation can be expedited by constructing a table of the form shown in Figure 14. Windows are cut in a paper representing the turn positions so that when this template is placed on the table the values appearing in the windows represent the field contributions at a distance from the center of the coil as indicated by the index mark. The double windows represent a turn whose radius falls between the two values of r in the table. For these values the mean of the two which appear is used. Note that as the index point moves

TABLE I

CALCULATED VALUES OF FIELD STRENGTH ON AXIS OF SINGLE TURNS OF $\frac{1}{8}$-INCH TUBING

(r AND x ARE $\frac{1}{16}$-INCH UNITS)

	r														
x	2	3	4	5	6	7	8	9	10	11	12	13	14	15	16
0	3.578	2.530	1.940	1.569	1.315	1.131	.992	.883	.796	.724	.664	.614	.570	.532	.499
1	2.828	2.219	1.789	1.486	1.265	1.099	.970	.868	.784	.716	.658	.608	.566	.529	.496
2	1.539	1.564	1.430	1.274	1.131	1.010	.908	.823	.751	.690	.638	.593	.553	.518	.488
3	.749	.981	1.040	1.013	.954	.886	.819	.757	.701	.651	.607	.568	.533	.502	.474
4	.386	.602	.723	.770	.772	.749	.716	.678	.639	.603	.568	.536	.507	.480	.456
5	.217	.378	.500	.574	.610	.619	.611	.594	.572	.548	.524	.500	.477	.455	.434
6	.132	.247	.349	.427	.476	.503	.514	.513	.505	.492	.477	.460	.444	.427	.410
7	.086	.168	.250	.319	.372	.407	.428	.439	.441	.437	.430	.420	.409	.397	.384
8	.059	.118	.182	.242	.291	.329	.356	.373	.382	.385	.385	.380	.374	.366	.358
9	.042	.086	.136	.186	.230	.267	.295	.316	.330	.338	.342	.342	.340	.336	.331
10	.031	.064	.104	.145	.183	.217	.245	.267	.284	.295	.303	.307	.308	.307	.305
11	.023	.049	.081	.115	.148	.178	.205	.227	.244	.258	.268	.274	.278	.280	.280
12	.018	.039	.064	.092	.120	.147	.172	.193	.211	.225	.236	.245	.251	.254	.256
13	.014	.031	.051	.075	.099	.123	.145	.165	.182	.197	.209	.218	.225	.230	.234
14	.011	.025	.042	.061	.082	.103	.123	.141	.158	.172	.184	.194	.202	.209	.213
15	.009	.020	.034	.051	.069	.087	.105	.122	.137	.151	.163	.173	.182	.189	.194
16	.008	.017	.029	.043	.058	.074	.090	.105	.120	.133	.144	.155	.163	.171	.177
17	.006	.014	.024	.036	.049	.063	.078	.091	.105	.117	.128	.138	.147	.155	.161
18	.005	.012	.021	.031	.042	.055	.067	.080	.092	.103	.114	.124	.133	.140	.147
19	.005	.010	.018	.026	.037	.047	.059	.070	.081	.092	.102	.111	.120	.127	.134
20	.004	.009	.015	.023	.032	.041	.051	.062	.072	.082	.091	.100	.108	.115	.122
21	.003	.008	.013	.020	.028	.036	.045	.055	.064	.073	.082	.090	.098	.105	.111
22	.003	.007	.011	.017	.024	.032	.040	.048	.057	.065	.073	.081	.089	.096	.102
23	.003	.006	.010	.015	.022	.028	.036	.043	.051	.059	.066	.073	.080	.087	.093
24	.002	.005	.009	.014	.019	.025	.032	.039	.046	.053	.060	.067	.073	.080	.085
25	.002	.005	.008	.012	.017	.022	.028	.035	.041	.048	.054	.061	.067	.073	.078
26	.002	.004	.007	.011	.015	.020	.025	.031	.037	.043	.049	.055	.061	.067	.072
27	.002	.004	.006	.010	.014	.018	.023	.028	.034	.039					
28	.001	.003	.006	.009	.012	.016	.021	.026	.030	.036					
29	.001	.003	.005	.008	.011	.015	.019	.023	.028	.032					
30	.001	.003	.005	.007	.010	.013	.017	.021	.025	.030					
31	.001	.002	.004	.006	.009	.012	.016	.019	.023	.027					
32	.001	.002	.004	.006	.008	.011	.014	.018	.021	.025					
33	.001	.002	.003	.005	.008	.010	.013	.016	.020	.023					
34	.001	.002	.003	.005	.007	.009	.012	.015	.018	.021					
35	.001	.002	.003	.005	.006	.009	.011	.014	.017	.020					
36	.001	.002	.003	.004	.006	.008	.010	.013	.015	.018					
37	.001	.001	.002	.004	.005	.007	.009	.012	.014	.017					
38	.001	.001	.002	.004	.005	.007	.009	.011	.013	.016					
39	.001	.001	.002	.003	.005	.006	.008	.010	.012	.015					
40	.000	.001	.002	.003	.004	.006	.008	.009	.011	.014					

TABLE II

CALCULATED VALUES OF FIELD STRENGTH ON AXIS OF SINGLE TURNS OF $\frac{3}{16}$-INCH TUBING

(r AND x ARE $\frac{1}{16}$-INCH UNITS)

x	r = 3	4	5	6	7	8	9	10	11	12	13	14	15	16	17
0	2.385	1.873	1.533	1.294	1.117	.983	.877	.791	.721	.662	.611	.568	.531	.498	.469
1	2.146	1.744	1.458	1.247	1.087	.962	.862	.780	.712	.655	.606	.564	.527	.495	.466
2	1.586	1.425	1.264	1.122	1.003	.903	.819	.748	.687	.636	.591	.552	.517	.487	.459
3	1.026	1.057	1.018	.953	.883	.816	.754	.699	.649	.606	.567	.532	.501	.473	.448
4	.634	.743	.781	.776	.751	.715	.677	.638	.602	.567	.535	.506	.480	.455	.433
5	.397	.515	.584	.616	.622	.613	.595	.572	.548	.523	.499	.476	.454	.434	.415
6	.257	.360	.435	.482	.507	.516	.515	.506	.493	.477	.460	.443	.426	.410	.394
7	.174	.256	.325	.377	.411	.431	.440	.442	.438	.430	.420	.409	.397	.384	.372
8	.122	.187	.246	.295	.332	.358	.375	.383	.386	.385	.381	.374	.367	.358	.348
9	.088	.139	.189	.233	.269	.297	.318	.331	.339	.343	.343	.341	.337	.331	.325
10	.066	.106	.147	.186	.219	.247	.269	.285	.297	.304	.308	.309	.308	.305	.302
11	.050	.082	.116	.149	.180	.206	.228	.246	.259	.268	.275	.279	.280	.280	.279
12	.039	.065	.093	.122	.149	.173	.194	.212	.226	.237	.245	.251	.255	.257	.257
13	.031	.052	.075	.100	.124	.146	.166	.183	.197	.209	.219	.226	.231	.234	.236
14	.025	.042	.062	.083	.104	.124	.142	.158	.173	.185	.195	.203	.209	.214	.217
15	.020	.035	.051	.069	.088	.105	.122	.138	.152	.164	.174	.182	.189	.195	.199
16	.017	.029	.043	.058	.074	.090	.106	.120	.133	.145	.155	.164	.171	.177	.182
17	.014	.024	.036	.050	.064	.078	.092	.105	.117	.129	.139	.147	.155	.162	.167
18	.012	.021	.031	.043	.055	.068	.080	.092	.104	.114	.124	.133	.140	.147	.153
19	.010	.018	.027	.037	.048	.059	.070	.081	.092	.102	.111	.120	.127	.134	.140
20	.009	.015	.023	.032	.042	.052	.062	.072	.082	.091	.100	.108	.116	.122	.128
21	.008	.013	.020	.028	.036	.045	.055	.064	.073	.082	.090	.098	.105	.112	.118
22	.007	.012	.018	.024	.032	.040	.049	.057	.065	.074	.081	.089	.096	.102	.108
23	.006	.010	.015	.022	.028	.036	.043	.051	.059	.066	.074	.081	.087	.093	.099
24	.005	.009	.014	.019	.025	.032	.039	.046	.053	.060	.067	.073	.080	.086	.091
25	.005	.008	.012	.017	.023	.028	.035	.041	.048	.054	.061	.067	.073	.079	.084
26	.004	.007	.011	.015	.020	.026	.031	.037	.043	.049	.055	.061	.067	.072	.077
27	.004	.006	.010	.014	.018	.023	.028	.034	.039	.045	.050	.056	.061	.066	.071
28	.003	.006	.009	.012	.016	.021	.026	.031	.036	.041	.046	.051	.056	.061	.066
29	.003	.005	.008	.011	.015	.019	.023	.028	.033	.037	.042	.047	.052	.057	.061
30	.003	.005	.007	.010	.013	.017	.021	.025	.030	.034	.039	.043	.048	.052	.057
31	.002	.004	.006	.009	.012	.016	.019	.023	.027	.031	.036	.040	.044	.048	.052
32	.002	.004	.006	.008	.011	.014	.018	.021	.025	.029	.033	.037	.041	.045	.049
33	.002	.003	.005	.008	.010	.013	.016	.020	.023	.027	.030	.034	.038	.042	.045
34	.002	.003	.005	.007	.009	.012	.015	.018	.021	.025	.028	.032	.035	.039	.042
35	.002	.003	.005	.006	.009	.011	.014	.017	.020	.023	.026	.029	.033	.036	.039
36						.010	.013	.015	.018	.021	.024	.027	.030	.034	.037
37						.009	.012	.014	.017	.020	.022	.025	.028	.031	.034
38						.009	.011	.013	.016	.018	.021	.024	.026	.029	.032
39						.008	.010	.012	.015	.017	.020	.022	.025	.027	.030
40						.008	.009	.011	.014	.016	.018	.021	.023	.026	.028
41						.007	.009	.011	.013	.015	.017	.019	.022	.024	.026
42						.007	.008	.010	.012	.014	.016	.018	.020	.023	.025
43						.006	.008	.009	.011	.013	.015	.017	.019	.021	.023
44						.006	.007	.009	.010	.012	.014	.016	.018	.020	.022
45						.005	.007	.008	.010	.011	.013	.015	.017	.019	.021
46						.005	.006	.008	.009	.011	.012	.014	.016	.018	.020
47						.005	.006	.007	.009	.010	.012	.013	.015	.017	.019
48						.004	.006	.007	.008	.010	.011	.013	.014	.016	.018

TABLE III

CALCULATED VALUES OF FIELD STRENGTH ON AXIS OF SINGLE TURNS OF $\frac{1}{4}$-INCH TUBING

(r AND x ARE $\frac{1}{16}$-INCH UNITS)

	r									
x	4	6	8	10	12	14	16	18	20	22
0	1.789	1.265	.970	.784	.658	.566	.496	.442	.398	.362
1	1.685	1.223	.950	.774	.651	.562	.493	.440	.397	.361
2	1.414	1.109	.894	.743	.632	.549	.485	.434	.392	.358
3	1.077	.952	.812	.695	.603	.530	.472	.424	.385	.352
4	.770	.782	.715	.637	.566	.505	.454	.412	.376	.345
5	.536	.624	.615	.572	.523	.475	.433	.396	.364	.336
6	.375	.491	.520	.507	.477	.443	.409	.378	.351	.326
7	.266	.384	.435	.444	.431	.409	.384	.359	.336	.314
8	.193	.301	.362	.385	.386	.375	.358	.339	.320	.301
9	.143	.237	.300	.333	.344	.341	.331	.318	.303	.288
10	.109	.189	.250	.287	.305	.309	.306	.297	.286	.274
11	.084	.152	.208	.247	.270	.279	.281	.277	.269	.260
12	.066	.123	.175	.213	.238	.252	.257	.257	.252	.246
13	.053	.101	.147	.184	.210	.226	.235	.237	.236	.232
14	.043	.084	.125	.160	.186	.204	.214	.219	.220	.219
15	.035	.070	.106	.139	.164	.183	.195	.202	.205	.205
16	.029	.059	.091	.121	.146	.164	.178	.186	.191	.193
17	.025	.050	.079	.106	.129	.148	.162	.172	.177	.181
18	.021	.043	.068	.093	.115	.133	.148	.158	.165	.169
19	.018	.037	.059	.082	.103	.120	.134	.145	.153	.158
20	.015	.032	.052	.072	.092	.109	.123	.134	.142	.148
21	.013	.028	.046	.064	.082	.098	.112	.123	.132	.138
22	.012	.025	.040	.057	.074	.089	.102	.113	.122	.129
23	.010	.022	.036	.051	.067	.081	.094	.105	.113	.120
24	.009	.019	.032	.046	.060	.074	.086	.096	.105	.113
25	.008	.017	.029	.041	.054	.067	.079	.089	.098	.105
26	.007	.015	.026	.037	.049	.061	.072	.082	.091	.098
27	.006	.014	.023	.034	.045	.056	.067	.076	.085	.092
28	.006	.012	.021	.031	.041	.051	.061	.071	.079	.086
29	.005	.011	.019	.028	.038	.047	.057	.065	.073	.081
30	.005	.010	.017	.025	.034	.043	.052	.061	.069	.075
31	.004	.009	.016	.023	.032	.040	.048	.057	.064	.071
32	.004	.008	.014	.021	.029	.037	.045	.053	.060	.066
33						.034	.042	.049	.056	.062
34						.032	.039	.046	.052	.058
35						.029	.036	.043	.049	.055
36						.027	.034	.040	.046	.052
37						.025	.031	.037	.043	.049
38						.024	.029	.035	.041	.046
39						.022	.027	.033	.038	.043
40						.021	.026	.031	.036	.041
41						.019	.024	.029	.034	.039
42						.018	.023	.027	.032	.036
43						.017	.021	.026	.030	.034
44						.016	.020	.024	.028	.033
45						.015	.019	.023	.027	.031
46						.014	.018	.022	.025	.029
47						.013	.017	.020	.024	.028
48						.013	.016	.019	.023	.026

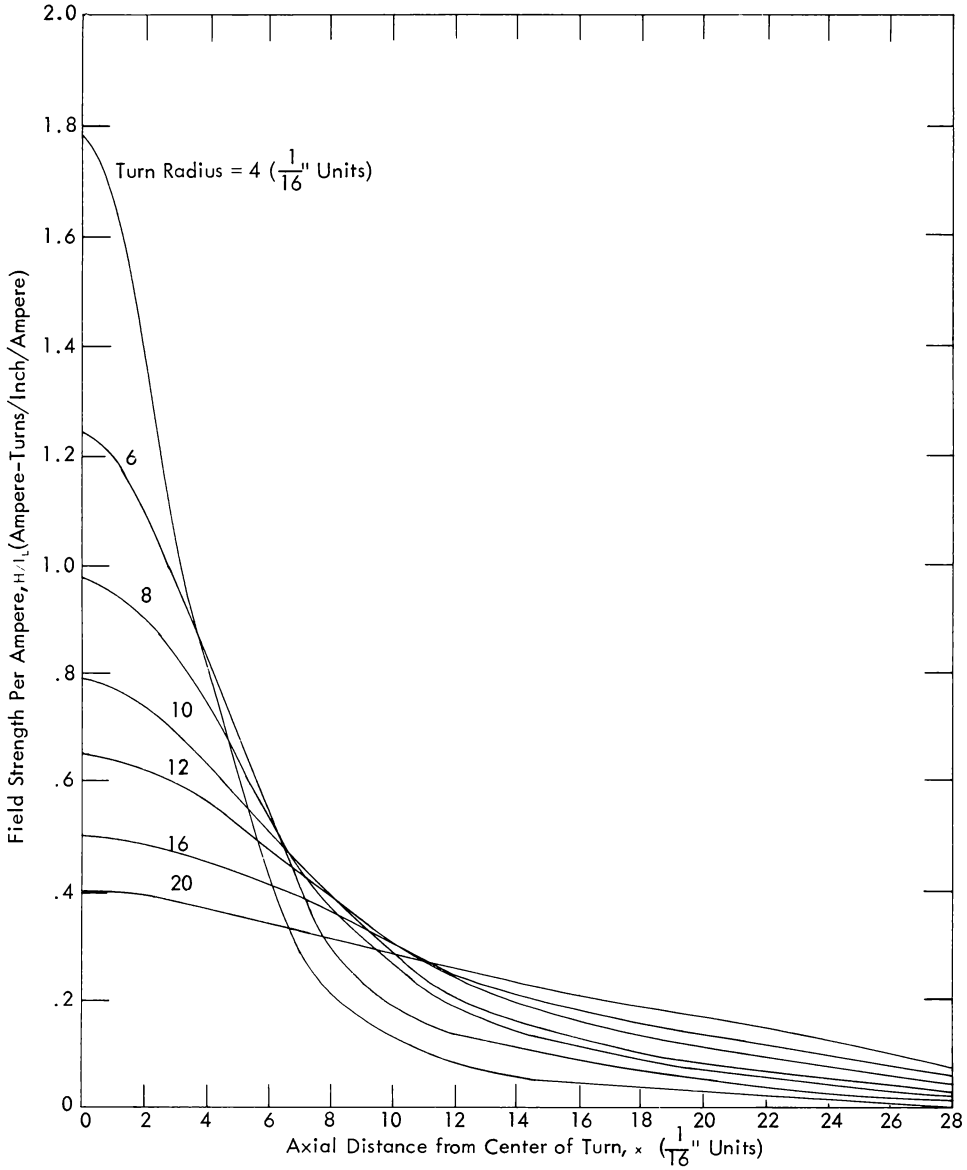

FIGURE 12

FIELD STRENGTH ALONG AXES OF VARIOUS DIAMETER TURNS OF $\frac{1}{4}$-INCH TUBING

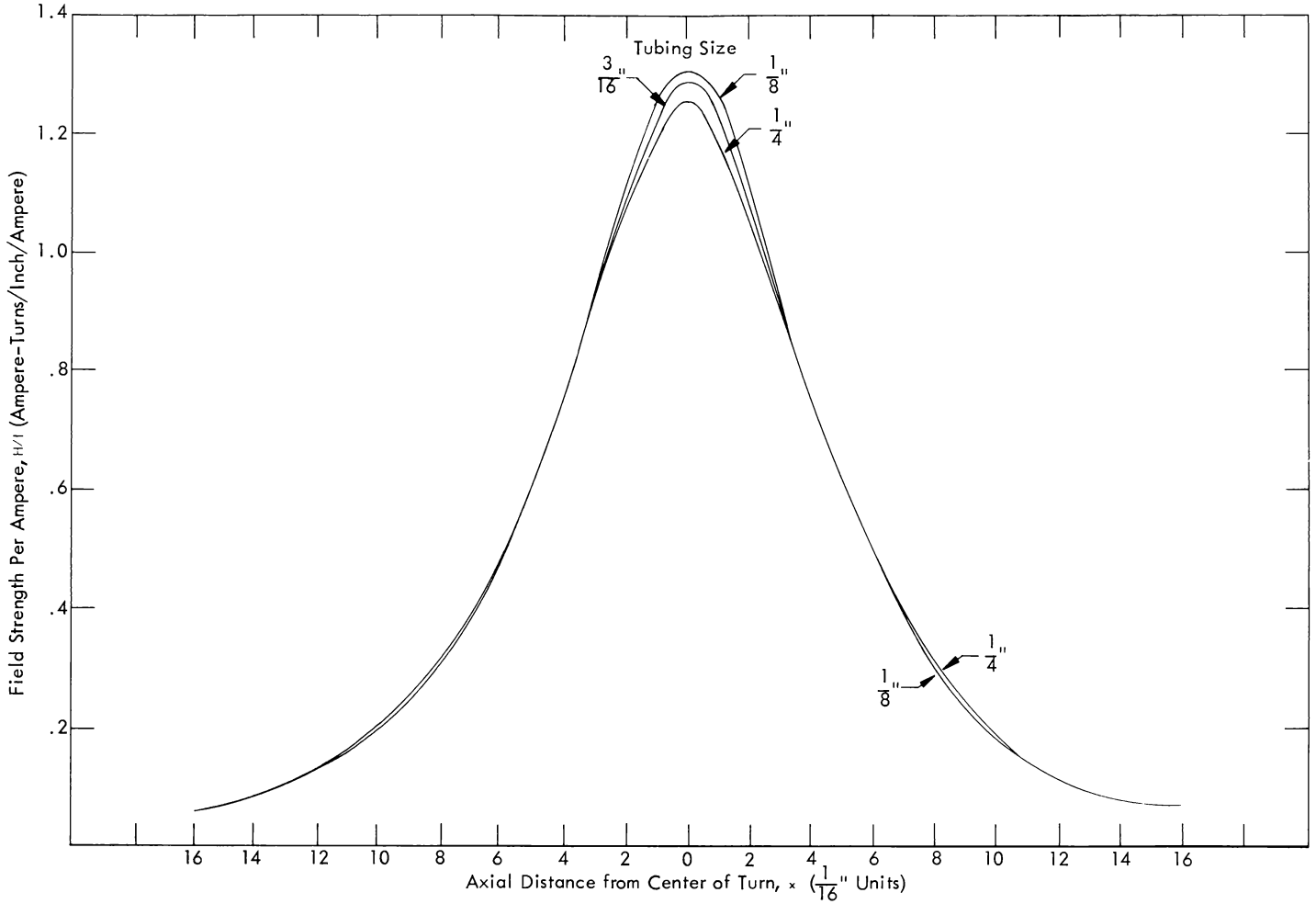

FIGURE 13

FIELD STRENGTH ALONG THE AXES OF $\frac{3}{4}$-INCH-DIAMETER TURNS OF VARIOUS SIZES OF TUBING

Turn Radius ($\frac{1}{16}$" Units)

Axial Distance, × ($\frac{1}{16}$" Units)	4	6	8	10	12	14	16	18	20	22
28	6	12	21	31	41	51	61	71	79	86
27	6	14	23	34	45	56	67	76	85	92
26	7	15	26	37	49	61	72	82	91	93
25	8	17	29	41	54	67	79	89	98	105
24	9	19	32	46	60	74	86	96	105	113
23	10	22	36	51	67	81	94	105	113	120
22	12	25	40	57	74	89	102	113	122	129
21	13	28	46	64	82	98	112	123	132	138
20	15	32	52	72	92	109	123	134	142	148
19	18	37	59	82	105	120	134	145	153	158
18	21	43	68	93	115	133	148	158	165	169
17	25	50	79	106	129	148	162	172	177	181
16	29	54	91	121	146	164	178	186	191	193
15	35	70	106	139	164	183	195	202	205	205
14	43	84	125	160	186	204	214	219	220	219
13	53	101	147	184	210	226	235	237	236	232
12	66	123	175	213	238	252	257	257	252	246
11	84	152	206	247	270	279	281	277	269	260
10	109	169	250	287	305	309	306	297	286	274
9	143	237	300	333	344	341	331	318	303	288
8	193	301	362	385	386	375	358	339	320	301
7	266	384	435	444	431	409	384	359	336	314
6	375	491	520	507	477	443	409	378	351	326
5 ◀	536	624	615	572	523	475	433	396	364	336
4	770	782	715	637	566	505	454	412	376	345
3	1077	952	812	695	603	530	472	424	385	352
2	1414	1109	894	743	632	549	485	434	392	358
1	1685	1223	950	774	651	562	493	440	397	361
0	1789	1265	970	784	658	564	496	442	398	362
1	1685	1223	950	774	651	562	493	440	397	361
2	1414	1109	894	743	632	549	485	434	392	358
3	1077	952	812	695	603	530	472	424	385	352
4	770	782	715	637	566	505	454	412	376	345
5	536	624	615	572	523	475	433	396	364	336
6	375	491	520	507	477	443	409	378	351	326
7	266	384	435	444	431	409	384	359	336	314
8	193	301	362	385	386	375	358	339	320	301
9	143	237	300	333	344	341	331	318	303	288
10	109	189	250	287	305	309	306	297	286	274
11	84	152	208	247	270	279	281	277	269	260
12	66	123	175	213	238	252	257	257	252	246
13	53	101	147	184	210	226	235	237	236	232
14	43	84	125	160	186	204	214	219	220	219
15	35	70	106	139	164	183	195	202	205	205
16	29	59	91	121	146	164	178	186	191	193
17	25	50	79	106	129	148	162	172	177	181
18	21	43	68	93	115	133	148	158	165	169

FIGURE 14

TEMPLATE PLACED OVER TABLE OF FIELD STRENGTH TO EXPEDITE CALCULATION OF COIL FIELD

upward the field below the center of the coil is being determined. In the example shown, the calculated field intensity 5/16 inch below the coil center is 1.76. The coil used here is Coil 64 shown in Figure 15. The calculated values of the field strength for this coil are also shown along with the values measured with the probe coil as discussed earlier.

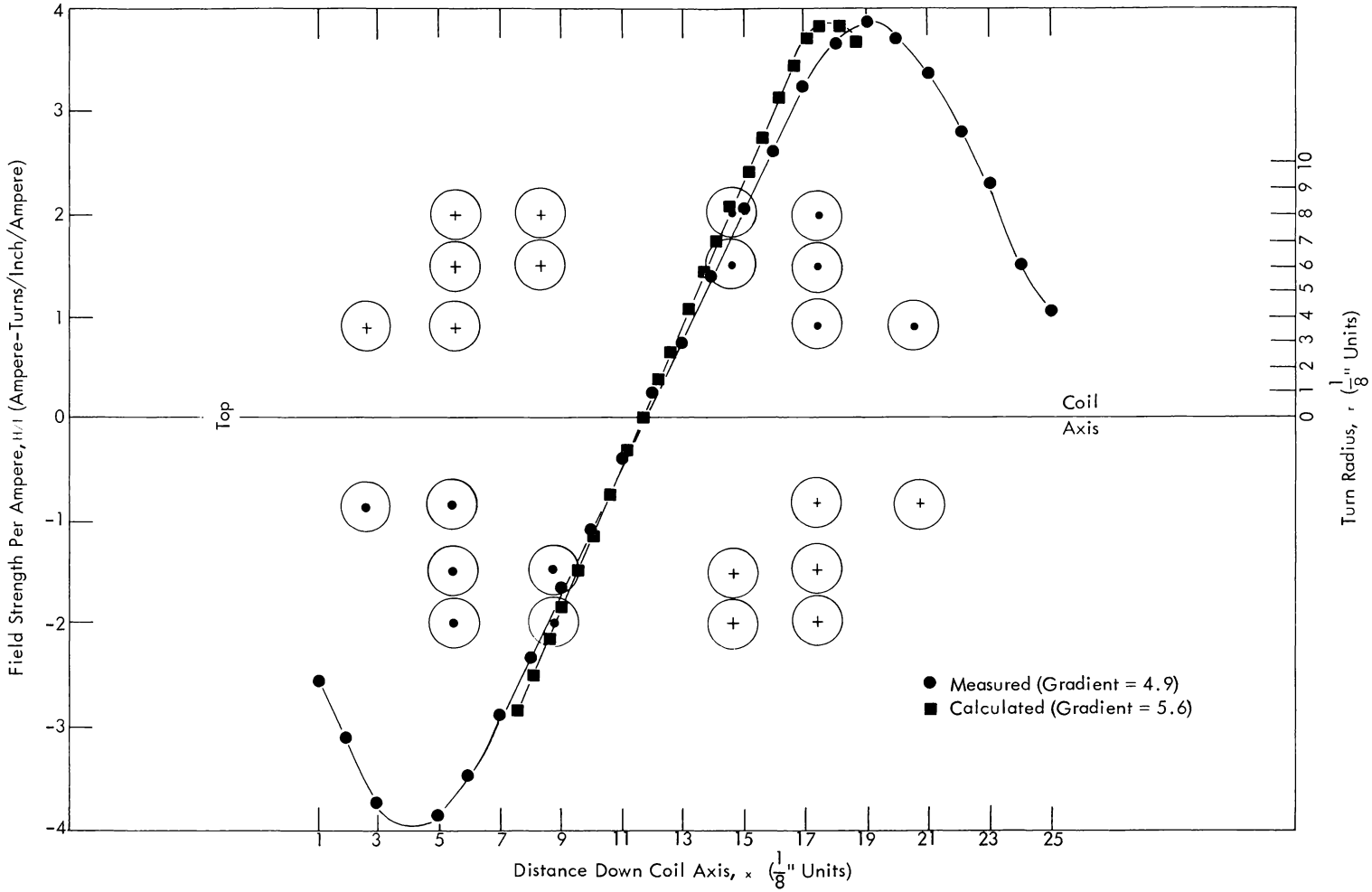

FIGURE 15

FIELD STRENGTH ALONG AXIS OF COIL 64 AND MEASURED COIL SHAPE

CHAPTER VII

CALCULATION OF GRADIENT

I FIELD DERIVATIVE

By differentiating Equation (22), an equation was obtained for the gradient of the field produced by a given turn:

$$G = -\frac{1}{2d}\left[\frac{r^2}{\left(r^2 + (d/2 + x)^2\right)^{3/2}} - \frac{r^2}{\left(r^2 + (d/2 - x)^2\right)^{3/2}}\right] . \tag{29}$$

Figure 16 is an evaluation of this equation for 1/4-inch tubing. Figure 17 shows a comparison of the values obtained from three different sizes of tubing.

Since the coil field is the sum of the fields of the separate turns, the coil gradient is the sum of the gradients. The field above and below a given turn is symmetrical and positive for bottom turns. Thus, the gradient is positive above a bottom turn and negative below it. The gradient for a top turn will be negative above the turn and positive below it.

II EFFECT OF NEGLECTING TUBING SIZE

Equation (22) reduces to the form

$$H/I_L = \frac{r^2}{2\left(r^2 + x^2\right)^{3/2}} , \tag{30}$$

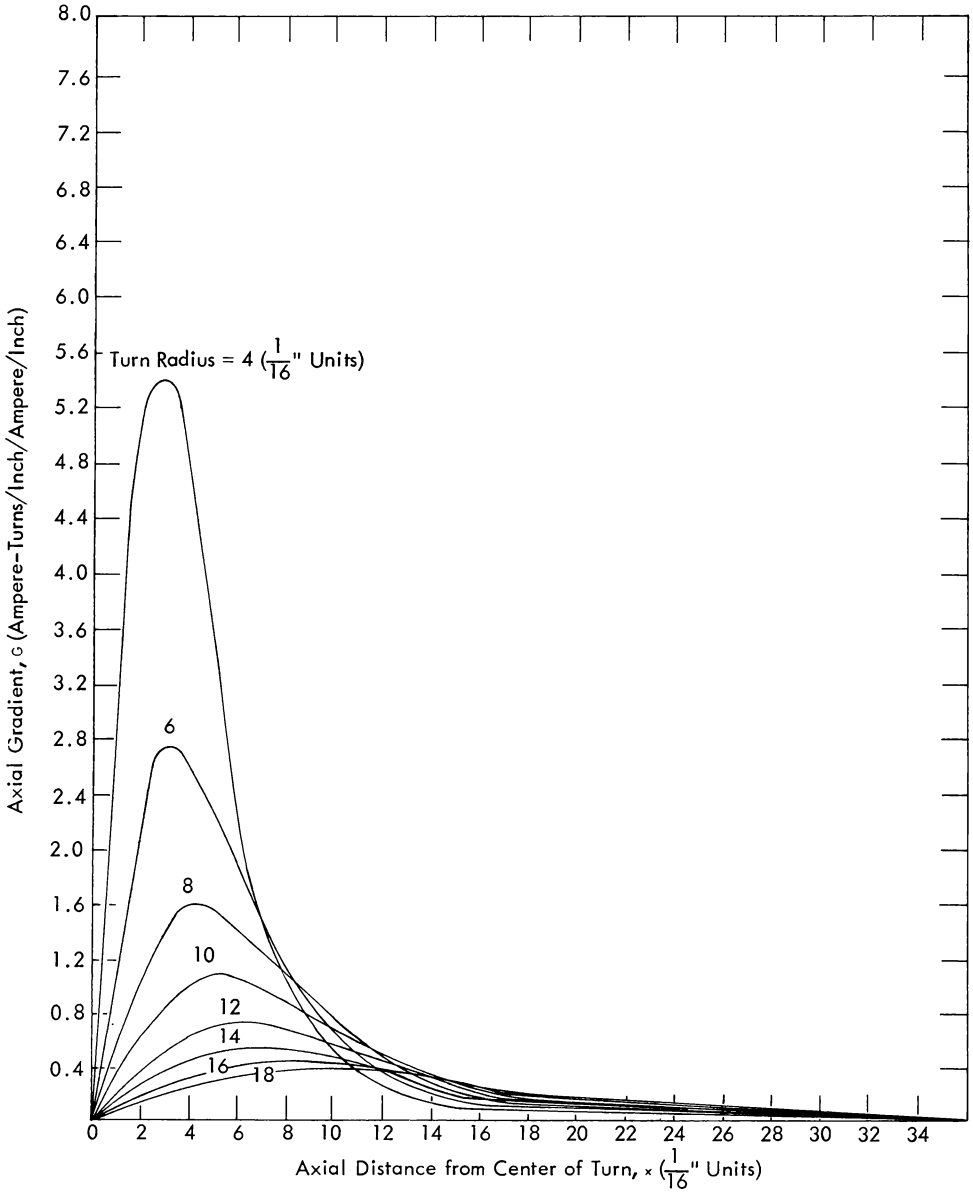

FIGURE 16

AXIAL GRADIENT FOR VARIOUS DIAMETER TURNS OF $\frac{1}{4}$-INCH-DIAMETER TUBING

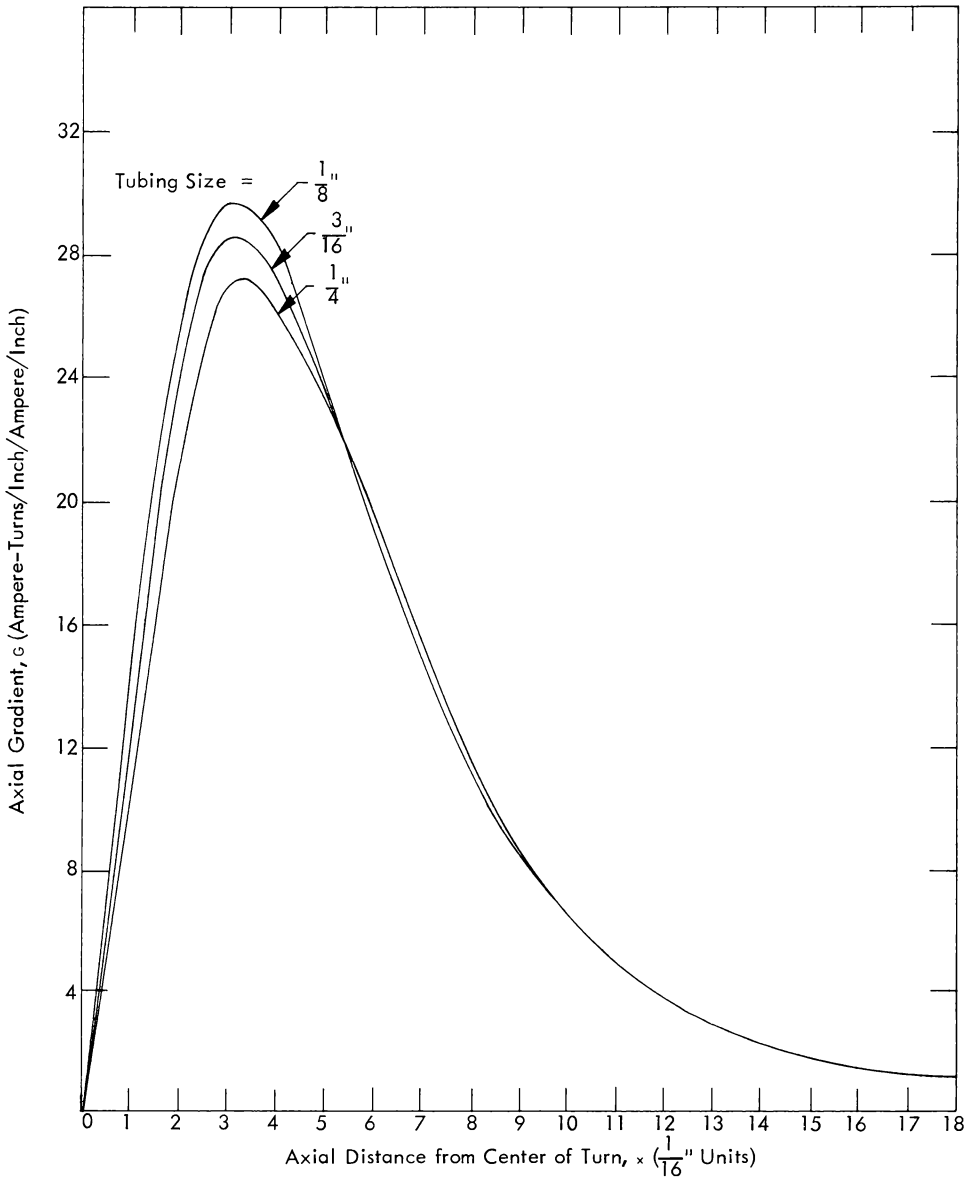

FIGURE 17

GRADIENT CONTRIBUTION FROM $\frac{3}{4}$-INCH DIAMETER TURNS OF DIFFERENT SIZE TUBING

when the effect of the tubing diameter is neglected.[15]

Differentiating we obtain,

$$G = \frac{\partial H/I_L}{\partial x} = -\frac{3}{2}\frac{xr^2}{\left(r^2 + x^2\right)^{5/2}} \quad . \tag{31}$$

In polar coordinates, where $r = v \sin\theta$, $x = v\cos\theta$ and $(x^2 + y^2)^{1/2} = v$, we have (neglecting sign)

$$G = \frac{3}{2}\frac{\cos\theta \sin^2\theta}{v^2} \quad , \tag{32}$$

or

$$v = \frac{1}{\sqrt{G}}\sqrt{\tfrac{3}{2}\cos\theta \sin^2\theta} \quad . \tag{33}$$

Table IV gives the last factor for various values of θ. This gives a convenient method of generating curves representing positions which yield the same value of gradient. Figure 18 shows these "isograds" in both polar and rectangular coordinates. Also shown are values of r and x obtained from Figure 16 for two values of G. These indicate that the effect of the tubing size is negligible in this range.

III USE OF ISOGRAD FIGURE

This figure can be used to determine the value of the specific gradient of a coil at any point along its axis. The contribution of a given turn of radius r at an axial distance x from the point is interpolated from the isograd figure. If

TABLE IV

VALUES OF FACTOR $\sqrt{\frac{3}{2}(\cos\theta - \cos^3\theta)}$ FOR USE IN CONSTRUCTING FIGURE 18

θ (Degrees)	$\sqrt{\frac{3}{2}(\cos\theta - \cos^3\theta)}$ $\frac{1}{16}$" Units
0	0.00
5	1.70
10	3.56
15	4.83
20	6.50
25	7.88
30	9.12
35	10.06
40	11.03
45	11.65
50	12.04
55	12.16
60	12.00
65	11.55
70	10.77
75	9.63
80	8.04
85	5.76
90	0.00

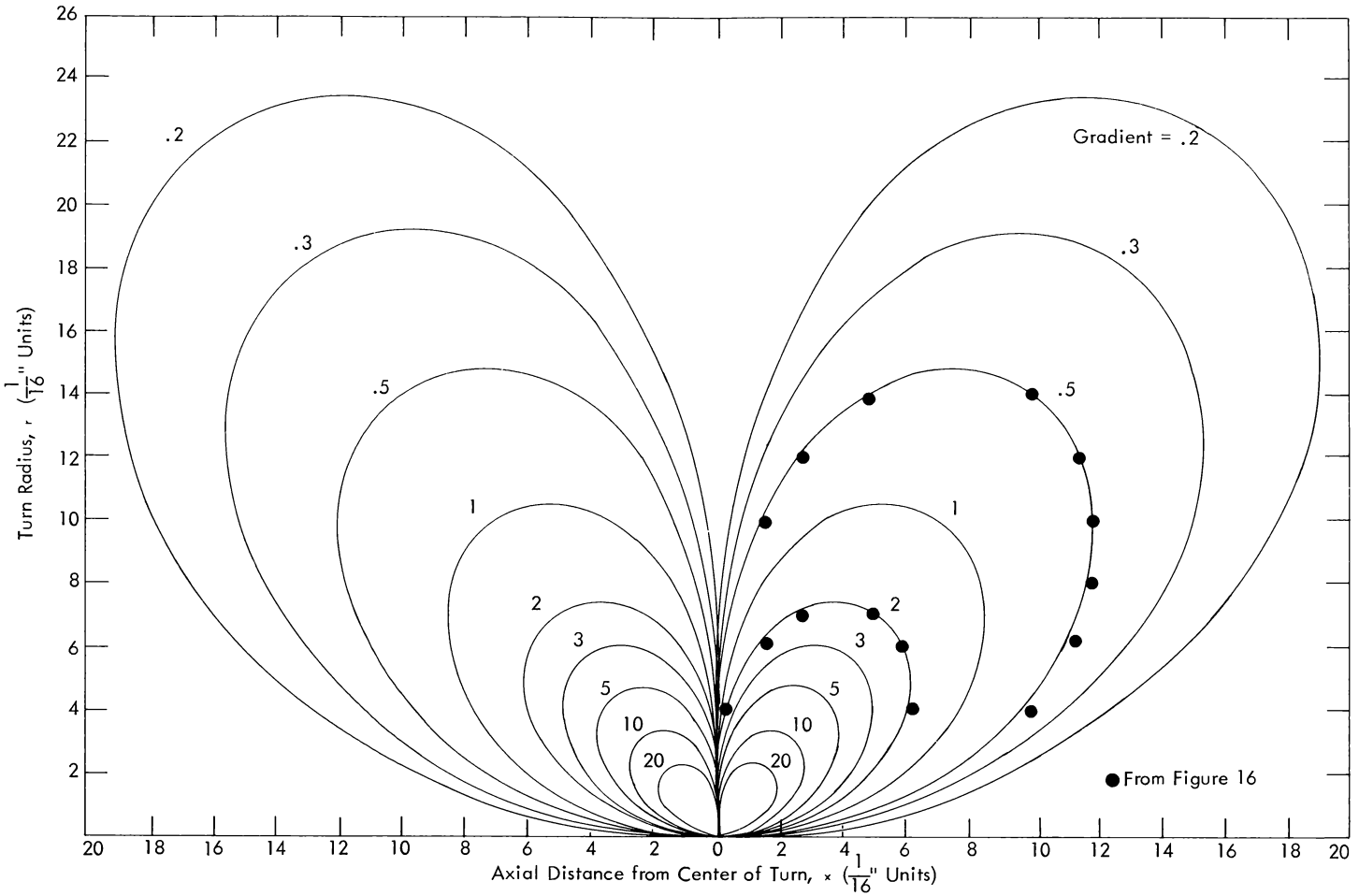

FIGURE 18

GRADIENT CONTRIBUTION AS A FUNCTION OF TURN POSITION

a top (reverse wound) turn lies above the point, its contribution is positive; but it detracts from the gradient for all points above the turn.

If it is desired to determine the gradient at several point along the coil axis, a clear plastic overlay can be marked with points representing the relative turns positions using the same scale for r and x as in Figure 18. The origin of the figure is made to coincide with any point on the overlay axis. The gradient at this point is the sum of the values interpolated at each turn position. A lower turn makes a positive contribution when falling on the right side of the figure and negative when on the left.

An average value of 5.5 was obtained for Coil 64 by this procedure which compares with the measured value of 4.9.

IV AVERAGE CONTRIBUTION

Figure 18 shows the positions in which turns will add most to the gradient at a given point along the axis of the levitation coil. However, for the purpose of design it is more desirable to consider the average gradient contribution over the distance occupied by the charge. For example, a turn placed in such a position as to give a maximum contribution at the null point might be above the level of the bottom of the charge so that it decreases the gradient at this point. The average gradient of the field strength function over a distance $x \pm M$ is given by:

$$\overline{G} \equiv \frac{H/I_L\ (x - M) - H/I_L\ (x + M)}{2M} , \tag{34}$$

where $H/I_L(x - M)$ is the value of Equation (29) at $x - M$. The axial length occupied by the charge would be $2M$. Figure 19 shows the values of $\bar{G}$ for 1/4-inch tubing with $2M$ equal to one inch. From this figure we may, by noting the values of r and x which give the same value of $\bar{G}$, construct Figure 20. This may be used to determine the turn positions which add the greatest amount to the over-all coil gradient. In the case of most coil designs where the gradient is constant over the length $2M$, Figure 20 and Figure 18 would give the same value for the gradient; but as pointed out before, Figure 20 is better suited for designing. A value of 5.5 for the average gradient of Coil 64 was also calculated by this method.

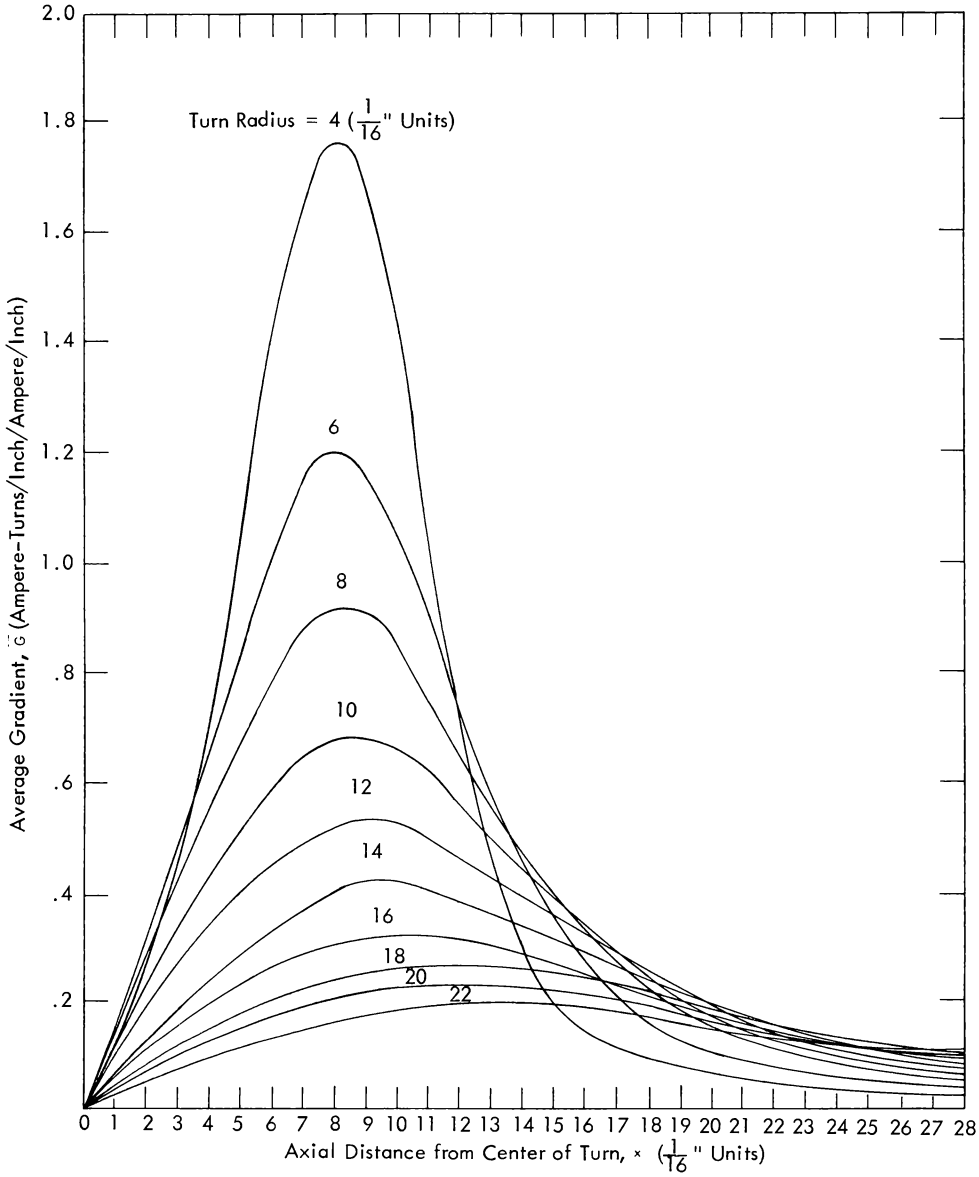

FIGURE 19

AVERAGE GRADIENT CONTRIBUTION OVER AN INTERVAL $\frac{1}{2}$-INCH ABOVE AND BELOW THE NULL POINT FOR VARIOUS TURN RADII OF $\frac{1}{4}$-INCH TUBING

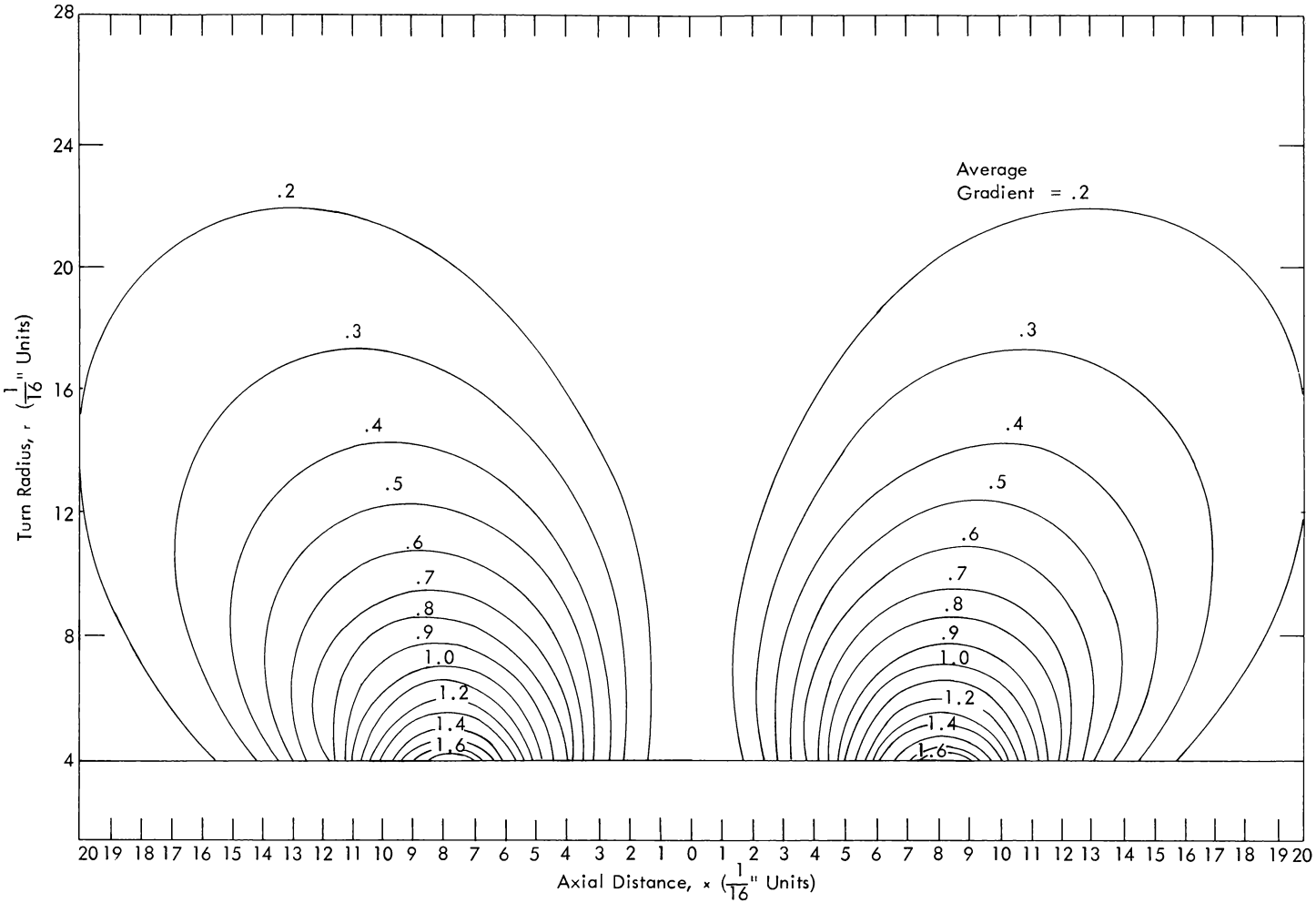

FIGURE 20

POSITION OF TURNS GIVING SELECTED VALUES OF AVERAGE GRADIENT $\frac{1}{2}$-INCH ABOVE AND BELOW NULL POINT

CHAPTER VIII

OTHER FACTORS IN COIL DESIGN

I TUBING SIZE

The diameter of the tubing used in the coil should be kept small to increase the number of turns which can be used in the high gradient positions. This is especially important when a multi-layer design is used or when power losses in the bus system are appreciable. The minimum size which can be used will depend on the amount of power which must be dissipated in the cooling water.

II NUMBER OF TURNS

Since the optimum heating efficiency is realized when the ratio of the square of the coil gradient to the coil resistance is largest, the choice of adding an additional turn to the coil design depends on its effect on the ratio of G^2 to the total tubing length. Usually, after several turns have been used in the design, this ratio does not change enough to be of any importance. For the size coils used in this study, five or six turns each in the top and bottom sections were found to be the optimum.

III PHYSICAL RESTRICTIONS

The location of the turns are limited by three physical restrictions. First, allowance must be made for inserting the charge. This opening can be at the top,

bottom, or sides of the coil. Although often more convenient, openings at the top or bottom will generally limit the use of turns in positions which add greatly to the coil gradient and thus reduce the heating efficiency. The bottom opening also decreases the liquid support. As seen in Figures 18 and 20, considerable opening can be left between the top and bottom sections without decreasing the axial gradient. This side loading can be used when maximum heating is necessary.

The other two restrictions deal with the coil fabrication. The coil must be made so that the leads can be brought out without interfering with the coil operation. The reversing connection from the top to bottom section should be short to minimize the coil resistance. Making this connection from the bottom turn of the top section to the top turn of the bottom section reduces this length and also reduces the problem of electrical discharge between the coil sections.

The second fabrication problem is due to the difficulty of bending tubing to small radii without flattening the tube and restricting water flow. By filling the tubing with dry sand before bending, 1/4-inch copper tubing can be bent to 1/4-inch internal radius. If it is necessary to have a smaller radius, a split washer can be brazed to the inside of the turn.

IV LIQUID SUPPORT

Since the levitating force is proportional to the field gradient and field strength, small diameter turns located just below the bottom tip of the melt will add to its support. In some cases, as with very light, high surface tension metals, the

tip support can be so great as to interfere with the pour of the molten metal. If the tip is stable at very low coil currents, the bulk of the liquid may fall before pouring begins at the tip, thus fouling the coil. This can be overcome by either opening up the bottom of the coil or placing a small "robber" coil under the levitation coil. This additional coil can be designed so its circuit can be closed, allowing it to act as a transformer secondary carrying currents induced by the levitation field. The field thus produced will be in such a direction as to counter the field near the bottom tip of the melt causing it to pour more easily.

The liquid metal may sometimes tend to overflow the sides of the coil between the upper and lower sections of the coil. This is especially true in the side-loading design. It then becomes necessary to reduce this spacing or add additional large diameter turns in this region.

CHAPTER IX

DISCUSSION

I ACCURACY OF METHOD

The accuracy of the power input equation and the field and gradient calculations is of the order of ten per cent. This is also the order of the error involved in measuring the actual dimensions of the coil. The turns will neither lie in a simple plane nor be of constant radius so that considerable estimation is involved in fixing the coil dimensions. The accuracy of this analysis is quite sufficient for the intended purpose of providing an understanding of the parameters involved in the design and performance of levitation melting coils at least with respect to the heating phenomena.

II LIQUID SUPPORT

Since the levitating force is equal to the product of the current in the charge and the spatial flux gradient, the observed linear axial gradient could probably be incorporated in a more thorough analysis of the liquid support. It may be necessary also to consider the radial gradients of the field in such an analysis. The equivalent resistance equation for the molten metal would probably contain shape factors that would depend essentially on the volume of the molten mass so long as the same general coil configuration is used since equal volumes of various molten metals will assume similar shapes.

III LARGE QUANTITIES

A thorough study of the levitation of molten metals would undoubtedly result in the ability to melt quite large quantities of the lighter metals. The process has been generally used for quantities of around five to twenty-five grams, but some cursory work with aluminum and beryllium has indicated that as much as several pounds of these metals could be levitated while molten.

IV OTHER COIL DESIGNS

The coil systems considered in this study are not the only types which might be used for levitation melting.[4-6] The only basic requirement for stable levitation is a high frequency field whose gradients are of such magnitude and direction as to counter the forces of gravity. At present, the coaxial, two-section coils used here appear to be the most desirable for their ease of fabrication and generally satisfactory operation.

V OTHER APPLICATIONS

The field calculation techniques presented here might be useful for other induction-heating calculations. For example, in the zone-refining process when it is desirable to maintain a narrow zone, reverse turns can be placed above and below the main coil to cause the field to decrease rapidly on either side of the zone. Figure 18 shows where the turns should be placed to be most effective, and Tables I, II, and III can be used to calculate the resulting field.

REFERENCES

REFERENCES

[1] Jenkins, A. E., C & EN, 38, August 21, 1961.

[2] Harris, B., and A. E. Jenkins, J. Sci. Instr., 36, (1959), p 238.

[3] Comenetz, G., and J. W. Salatka, J. Electrochemical Soc., 105, (1958), p 673.

[4] Fogel', A. A., Izvest, Akad. Nauk SSSR. OTN; Metall. i Toplivo, 2, (1958), p 24.

[5] Wroughton, D. M., E. C. Okress, P. H. Brace, G. Comenetz, and J. C. R. Kelly, J. Electrochemical Soc., 99, (1952), p 205.

[6] Ageev, N. V., A. A. Fogel', T. A. Sidorova, and V. A. Trapeznikov, Russian J. App. Chem. in English Translation, 33, (1960), p 330.

[7] Okress, E. C., D. M. Wroughton, G. Comenetz, P. H. Brace, and J. C. R. Kelley, J. App. Physics, 23, (1952), p 545.

[8] Slater, W. J., J. W. Barton, and R. Taggart, Sci. & Industry, 7, (1960), p 89.

[9] Scheibe, W., Metall, 7, (1953), p 751.

[10] Blade, J. C., J. W. H. Clare, and H. J. Lamb, J. Inst. of Metals, 88, (1959-1960), p 365.

[11] Weisberg, L. R., Rev. Sci. Instr., 30, (1959), p 135.

[12] Begley, R. T., G. Comenetz, P. A. Flinn, and J. W. Salatka, Rev. Sci. Instr., 30, (1959), p 38.

[13] Polonis, D. H., R. G. Butters, and J. G. Parr, Research, 7, (1954).

[14] Tudbury, C. A., Basics of Induction Heating, 1, John F. Rider Publisher, Inc., 1960, p 52.

[15] Eshbach, O. W., Handbook of Engineering Fundamentals, Second edition, John Wiley & Sons Inc., 1957, p 9-24.

SYMBOLS AND NOMENCLATURE

Symbol	Meaning	Units
a_1, a_2, a_3	Factors depending on shape of workpiece	---
B	Flux density	webers/inch^2
C	Capacitance	farads
d	Solenoid length (tubing size)	inches
D	Workpiece diameter	inches
D_M	Molten metal density	pounds/inch^3
E	Electric potential	volts
E_0	Voltage across tank circuit	volts
E_w	Voltage induced on workpiece	volts
f	Frequency	cycles/second
G	Specific axial field gradient	ampere-turns/inch/ampere/inch
$\overline{G}$	Average axial gradient	ampere-turns/inch/ampere/inch
h	Levitated liquid metal height	inches
H	Field strength	ampere-turns/inch
I_L	Coil current	amperes
I_w	Eddy current in workpiece	amperes
K	Frequency efficiency coefficient	---
L_w	Effective inductance of workpiece	henrys

Symbol	Meaning	Units
M	Fixed axial length (half of workpiece length)	inches
N	Number of coil turns	---
P_s	Pressure due to surface tension	pounds/inch^2
P_w	Power input to workpiece	watts
R	Resistance	ohms
R_{EQ}	Equivalent (or reflected) resistance	ohms
R_w	Effective resistance of workpiece	ohms
r_s	Radius of curvature of liquid metal surface	inches
r_B	Radius of curvature at bottom of levitated liquid	inches
r_T	Radius of curvature at top of levitated liquid	inches
r_w	Radius of workpiece	inches
r	Radius of coil turn	inches
S_1, S_2	Factors depending on shape of workpiece	---
t	Time	seconds
v	Radius vector for polar notation	inches
x	Axial distance	inches
Δx	Finite increment of axial distance	inches
X_w	Effective inductive reactance of workpiece	ohms
γ	Surface tension	pounds/inch
δ	Reference depth	micro-inches
θ	Angular displacement for polar notation	degrees

Symbol		Units
μ	Permeability	---
ρ	Resistivity	microhm-inches
ϕ	Total flux	webers
ω	Angular frequency	radians/second
ω_o	Resonant angular frequency	radians/second